8-16-2013

Using Analytic Techniques to Resolve Numerical Issues in a Pseudo Spectral Solver for a Black Hole Scalar Field

Eugene Munro

Using Analytic Techniques to Resolve Numerical Issues in a Pseudo Spectral Solver for a Black Hole Scalar Field

Eugene Munro

A Thesis Submitted in Partial Fulfillment of the Requirements for the Degree of Master of Science *in* Applied Mathematics

School of Mathematical Sciences

College of Science

Rochester Institute of Technology

Rochester, NY

August 16, 2013

Thesis Supervisor: Josh A. Faber, School of Mathematical Sciences

Thesis Supervisor: Tony A. Harkin, School of Mathematical Sciences

Thesis Supervisor: Chris Wahle, School of Mathematical Sciences

Contents

Abstract

Of all the events in our Universe, the merger of two Super Massive Black Holes is thought to be the most explosive and energetic cosmic event since the Big Bang. Our modern understanding about the nature of such an event spawns from the brilliant mind of Albert Einstein in his General Theory of Relativity. By viewing gravity as an effect of the deformation of spacetime by a massive object, we can understand the nature of black holes. The mass equivalent to ten billion of our suns compressed into a single point in space, a singularity, warps the fabric of our universe to its limits.

In this paper, we will solve the Hamiltonian constraint describing a curved general relativistic spacetime to find initial data describing how a black hole exists in vacuum. This has been done before by other researchers [1], and we will be adapting our own methods to an existing pseudo spectral Poisson solver [3]. The need for this adaptation arises from improper numerical handling, done by pseudo spectral-methods, of a large part the Hamiltonian constraint equation due to the presence of the black hole singularity. To resolve a portion of this issue up to a given order, we will determine *irregular terms* by executing a polynomial expansion on the Hamiltonian constraint, analytically solving the troublesome components of the equation and subtracting those out of the numerical process. This technique will increase the equation's differentiability and allow the numerical solver to run more efficiently.

We will cover all the calculations needed to describe one black hole with arbitrary spin and linear momentum. Our process is easily expanded into cases with n black holes [2], which we will show in chapter 2. We will implement a spherical harmonic decomposition of the black hole conformal factor, using them as basis functions by which to further expand and dissect the Hamiltonian Constraint equation. In the end, the expansion and subtraction method will be done out to the order of r^4, where r is the spherical radius assuming the black hole is at the coordinate origin, making the Hamiltonian equation, which, unaltered, is a C^2 equation, become a C^7 equation. Smoothing the Hamiltonian improves numerical precision, especially near the BH where the most interesting physics occurs. The method used in this paper can be further implemented to higher orders of r to yield even smoother conditions. We will test the numerical results of using this method against the existing solver that uses the publicly available `Lorene` numerical libraries and programmed in C.

Chapter 1

Preliminaries

This chapter gives a brief overview of the mathematical objects we will be dealing with in this paper, as well as some of their physical understandings and implications. We will also introduce what a black hole is, how we can study such an object and where the equations we will use come from.

1.1 Black Holes

A black hole is the end product of a massive star that has collapsed under its own gravitational force at the end of its life. Instead of the star exploding and ejecting all of its material composition into space, a substantial fraction of its mass collapses in on itself infinitely to a single point. This creates a gravitational singularity where the region of spacetime has infinite curvature, or infinite gravitational force. The gravity is so strong that light cannot escape its pull once it goes beyond the event horizon; this is why we are unable to actually see a black hole. They are observable only by noting the action of visible bodies, such as stars or gas in orbit close enough to know that there must be an immensely massive object present, even if we cannot see the object directly. No other known object in the universe has a more dramatic effect on spacetime than a black hole.

Black holes can grow by colliding with, and thereby consuming, other objects. It is widely believed that the center of every galaxy houses a supermassive black hole that has the mass of $10^5 - 10^9\ M_\odot$. Many believe that while they seem to hold a lot of

destructive force, black holes might play a critical role in the formation of galaxies. They have the largest gravitational effect of any object in the known universe. For a static (non-spinning) black hole, the entirety of its mass is contained at a single point, whereas for a spinning black hole its mass exists as a ring shaped singularity. Both can be shown to have zero volume. Astonishingly, the center of a black hole can then be thought to also have infinite density.

However mysterious these cosmological objects may seem, we can say they only have three independent parameters: mass, angular momentum and electrical charge. Using these parameters we can study some physical aspects of black holes because these traits are visible outside of the event horizon. Specifically for this paper, we will study how black holes affect the spacetime around them. Setting up this initial data of how the geometry of spacetime is shaped around one or multiple black holes is the first step in evolving a merger of two or more of these cosmic beasts, and recreating the largest and most violent event in our universe; an event that pushes the bounds of modern physics to its limits.

1.2 Spacetime

In the last section the term spacetime was used repeatedly and we need a clear idea of what that is. Spacetime is what the name implies, the unified concept of three dimensional space with time, thus creating a four dimensional system that locates an object with the spacial coordinates of its position and the time at which it was there. All physical events take place in spacetime and it is independent of any observer.

Without getting too in depth with all the concepts that spacetime involves, a simple way to understand spacetime is to think of yourself as a point that moves around in space as time progresses linearly (on a graph, time is the vertical axis). This concept is an object known as a *world line* and all physical objects or events follow a world line that exists within another object known as a *light cone*. An example of a world line is the orbit of the Earth; in space it is an ellipse, while in spacetime it is a helix spiraling upwards.

The concept of world lines is important in the visualization of spacetime, but we can't think of massive objects like planets, or even people because massive objects curve

the spacetime around themselves and thus don't travel on pure paths called *geodesics*. More specifically, geodesics are paths through spacetime that optimize the *proper time* between the beginning and end of the path, i.e. taking the most direct route (locally). A massless particle in motion, known as a *test particle*, will always follow a geodesic. With a given initial position and velocity of a test particle, the geodesic equation will be affected by the *spacetime metric*. This metric is a 2^{nd} degree tensor that describes the coordinate acceleration of a test particle in a given space. If the space is flat then the particle will travel in what appears to be a straight line, but if the space is curved, as it is in the presence of mass and energy, then test particles travel along the curves of space itself. Figure 1 shows the geodesic paths taken in curved and flat region of space around a massive object. As seen in the path from C to D, the effect of "free-falling" for the test particle traveling along that path is simply that particle following a geodesic curve! The *gravity well* in Figure 1 pales in comparison to that of a black hole where the well is infinitely deep.

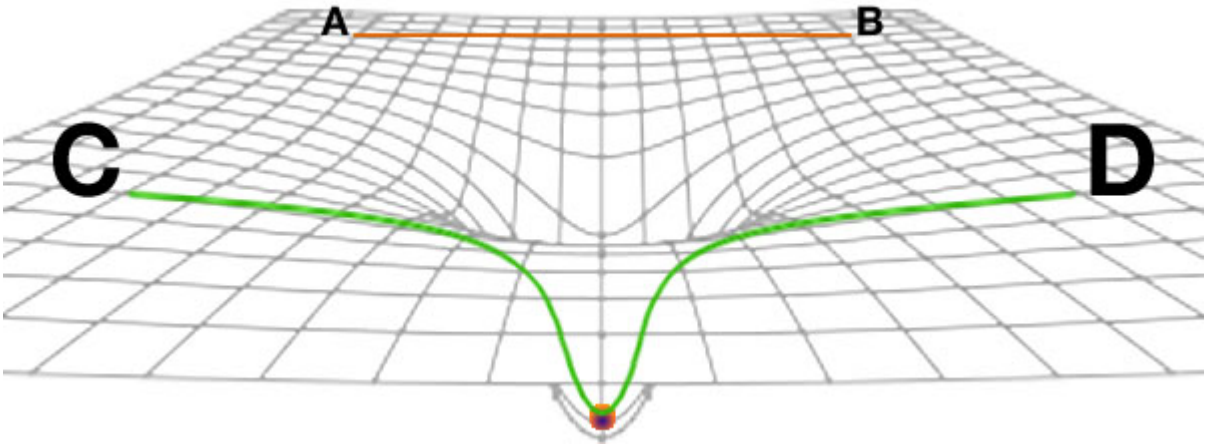

Figure 1. Image credit: http://www.physicsforums.com/showthread.php?t=400147

1.3 Tensors

Tensors are geometrical objects that create a linear map between vectors, scalars and other tensors. Operations such as dot product and cross product are well defined. The rank of a tenor is based on the dimension of the tensor. A vector would be a tensor of rank 1, while a metric, $g_{\mu\nu}$, is a tensor of rank 2. The extrinsic curvature tensor we will be dealing with is also of rank 2. The rank (also degree or order) of a tensor is the

dimensionality of the array needed to represent it, or equivalently, the number of indices needed to label a component of that array; so a second rank tensor is a matrix.

When an operator, such as a derivative $\frac{\partial}{\partial x^\mu}$, is applied to a tensor one must pay close attention to the indices and whether they are *covarient* (up), or *contravarient* (down), $\mathcal{T}^\mu$ vs $\mathcal{T}_\mu$ respectively. If the index is in a denominator, like with the derivative, then it is considered as a down index. Now it is important to note these, first because the number of up and down indices on both sides of an equation must agree, and secondly repeated indices indicate a summation (generalized dot product) and will always appear as an up/down pair. By standard conventions the index labels for these are arbitrarily picked, so summation indices are also called "dummy" indices. Basic linear algebra is implemented in tensor equations, the only tricky aspect to them is figuring out how many equations are actually captured in the one equation.

The only tensorial equation we see in this paper comes from the momentum constraint on the extrinsic curvature tensor.

Momentum Constraint

An important equation for our study comes from the momentum constraint on the extrinsic curvature tensor. The constraint generalizes the idea that momentum is a conserved quantity.

A second rank tensor, which represents the extrinsic curvature, is a large part of this paper. The extrinsic curvature tensor, $K_{\mu\nu}$, contains information about the spacetime curvature metric and how it warps due to the embedding of the spacetime surface. Basically, it represents a kind of acceleration in spacetime due to momentum and spin of a black hole or any other mass. However, since a black hole exists at only one point in space, the extrinsic curvature tensor describes the otherwise vacuum spacetime around that single point. Momentum is conserved through the actual warping of spacetime around a black hole.

The constraint can be expressed by the following tensor equation

$$\nabla_\mu K^{\mu\nu} = 0.$$

Since $K_{\mu\nu}$ is a 3x3 matrix, this one equation is actually 3 that can be seen if we change this equation into the following form

$$\nabla \cdot \overleftrightarrow{K} = (0,0,0)^T.$$

This equation now treats K as a matrix and T represents the transpose of the 0 vector. The revised equation reads as the generalized divergence of K is zero in all directions.

1.4 Einstein's Equations

First published in 1915 as a tensor equation, Einstein's Field Equations equate local spacetime curvature to the local energy and momentum within that spacetime. This tensor equation yields a set of 10 equations that describe the fundamental effect of gravitational force as a result of spacetime curvature by the presence of matter and energy. The field equations are basically used to determine the spacetime geometry of a space with known mass−energy and linear momentum. With the knowledge of the spacetime geometry we can determine the geodesic equations that govern particle and radiation paths, as well as orbital paths. The field equation can be written as follows:

$$\mathcal{R}_{\mu\nu} - \frac{1}{2} g_{\mu\nu}\mathcal{R} + g_{\mu\nu}\Lambda = \frac{8\pi G}{c^4}\mathcal{T}_{\mu\nu},$$

where $\mathcal{R}_{\mu\nu}$ is the Ricci curvature tensor, $\mathcal{R}$ the scalar curvature, $g_{\mu\nu}$ the metric tensor, Λ is the cosmological constant, G is Newton's gravitational constant, c the speed of light in vacuum, and $\mathcal{T}_{\mu\nu}$ is the stress−energy tensor. $G_{\mu\nu} = \mathcal{R}_{\mu\nu} - \frac{1}{2} g_{\mu\nu}\mathcal{R}$ is known as the Einstein Tensor. When written out, the field equations are a system of 10 coupled, nonlinear, hyperbolic−elliptic partial differential equations. The 10 equations arise from the fact that the set of 4x4 tensors are symmetric and thus have 10 independent components. As well as obeying local energy−momentum conservation, the field equations reduce to classical Newtonian physics in terms of gravitation when the gravitational field is weak and velocities are much less than the speed of light.

1.5 The Hamiltonian

In Hamiltonian Mechanics, a system is described by a set of canonical coordinates, $\mathbf{r} = (\mathbf{q}, \mathbf{p})$ where each component, $\mathbf{q_i}, \mathbf{p_i}$ is indexed to some coordinate system. Each canonical point describes the physical system at that point, so $\mathbf{q_i}$ could be a Cartesian location of the point and $\mathbf{p_i}$ would then be the momentum at that point. The time evolution is uniquely defined by Hamilton's equations:

$$\frac{d\mathbf{p}}{dt} = -\frac{\partial \mathcal{H}}{\partial \mathbf{q}}$$
$$\frac{d\mathbf{q}}{dt} = +\frac{\partial \mathcal{H}}{\partial \mathbf{p}}$$

The Hamiltonian, $\mathcal{H}(\mathbf{q}, \mathbf{p}, t)$, represents the total energy in a system. In a closed system the Hamiltonian would equal the sum of all the kinetic and potential energy.

1.6 Elliptic PDE

An elliptic partial differential equation is a second order equation of the general form,

$$Au_{xx} + 2Bu_{xy} + Cu_{yy} + Du_x + Eu_y + F = 0$$

that satisfies the condition $B^2 - AC < 0$ (we assume that $u_{xy} = u_{yx}$).

The Laplace and Poisson equations are the simplest examples of Elliptic PDEs. In this paper we will be solving a nonlinear Poisson equation, which simplifies to Laplace's equation when the right hand side is 0.

$$\left(\frac{\partial^2}{\partial x^2} + \frac{\partial^2}{\partial y^2} + \frac{\partial^2}{\partial z^2}\right)\varphi(x, y, z) = f(x, y, z, \varphi).$$

Solving this equation will tell us how some object or function is accelerating at any point in space. Some nonlinear PDEs are difficult to solve since the evolution of the system depends on the state of the system itself continuously. There are many methods for solving nonlinear systems, both analytically and numerically. The initial data problem

we will solve is one that cannot be represented by a closed analytic solution with our current knowledge. We will be building off of a pseudo spectral code that solves a Poisson equation for the gravitational potential around a BH. In an attempt to improve the working model, we will show the successes, failures and reaches of extending the adaptive method we put forth in this paper.

1.7 Current Numerical Process

Pseudo spectral-methods (PSMs) are a class power numerical techniques best suited for solving PDEs. The standard PSM calls on the orthogonality of the Fourier Series and Chebyshev polynomials and uses them as basis functions by which to represent and solve a desired function. The method is known for its exponential convergence and versatility, making PSMs a leading choice for a numerical solver. However, when applied to the initial BH data problem in this paper, the method runs into issues due to the puncture at the BH location. Much work has been done to remap a coordinate system and domain just so PSMs could be used, but there is no getting around numerical failings when dealing with a singularity. The error results reflect Gibbs phenomena, though modified with spherical harmonics in place of Fourier Series approximation.

Problems with the method

Virtually any conceivable numerical PDE solver will run into issues when dealing with a singularity in the domain, but the issues caused by PSMs are known and tractable under the right conditions. As a result of built in infrastructure, the pseudo spectral code only allows for certain (regular) modes to be used to represent a give solution. Regularity is based on the pairing of basis modes with powers of r within summation series. When the order of a given mode and it associated power of radius are both even or both odd, then the term is considered regular; otherwise it is called irregular.

This constraint on which terms are allowed weakens the solver since the Hamiltonian equation we are solving has an irregular component. Unfortunately the benefits of this restriction outweigh the benefits of allowing for irregular mode expansions within the numerical process. Simply allowing for irregular mode terms would create greater

problems when solving for both regular and irregular terms. Thus the resulting approximations are ill fitting for these irregularities in a similar sense of using odd polynomials to approximate an even function. The errors produced by this mismatching hinder the exponential convergence of PSMs and the method takes on a power law convergence instead.

Here, we have devised a way of locating irregular terms analytically and resolving a portion of this issue by exploiting certain aspects of the Hamiltonian Equation and the properties of BHs. Our goal is to attain better data near the singularity than previous PSMs have been able to accomplish by properly handling irregularities up to a desired order of accuracy.

Chapter 2

Initial Data for a Black Hole

2.1 Setting up the Problem

The Hamiltonian constraint in General Relativity is a nonlinear elliptic partial differential equation for the scalar field, Ψ,

$$\nabla^2\Psi + \frac{1}{8}K_{ab}K^{ab}\Psi^{-7} = 0. \tag{2.1}$$

Here, $\nabla^2 = \Delta$ is the Laplacian in spherical coordinates. The extrinsic curvature tensor, K_{ab}, is subject to the following momentum constraint

$$\nabla_a K^{ab} = 0. \tag{2.2}$$

Where ∇_a is a tensorial derivative operator.

In order to implement our numerical scheme effectively, we need to take our domain in which the black hole exists to be all of space, i.e. infinity. Since we cannot evaluate an infinite number of grid points, and expect the gravitational effects of a black hole to become asymptotically flat and negligible as one approaches an infinite distance away from the singularity we compactify our domain. In fact, the pseudo spectral numerical scheme we use requires grid points between -1 and 1, so we *must* compactify our numerical domain. We first redefine our scalar field by the following substitution,

$$\Psi = u + 1 + \frac{m_1}{2r_1} + \frac{m_2}{2r_2} + \frac{m_3}{2r_3} + ... + \frac{m_n}{2r_n}. \tag{2.3}$$

The newly introduced field u is continuous everywhere, including the center of the BH.

Here we have described a series of n isolated, stationary BHs in isotropic coordinates, where m_n represents the mass of the nth BH and r_n is the distance away a point is from the nth BH. This paper deals with only one BH, thus we have $\forall\ n > 1, m_n = 0$. Taking the Laplacian of this solution we see a very nice simple relation

$$\Delta\Psi = \Delta u + \Delta(1) + \Delta(\frac{m}{2r})$$

$$\Delta\Psi = \Delta u$$

This simple form arises since $\frac{1}{r}$ is an exact solution for the Laplacian in spherical coordinates. Substituting our new expression into the Hamiltonian thus becomes,

$$\nabla^2 u = -\frac{1}{8}K_{ab}K^{ab}(1 + \frac{m}{2r} + u)^{-7}$$

Simplifying further, we achieve the following form which has a nice polynomial expansion.

$$\nabla^2 u = -\frac{16r^7}{m^7}K_{ab}K^{ab}\left(1 + \frac{2r}{m}(1+u)\right)^{-7} \tag{2.4}$$

For the sake of clearer notation and computational simplicity later on, we let $\bar{u} = u + 1$ and note that $\nabla^2\bar{u} = \nabla^2 u$. Now we perform the polynomial expansion for $(1 + \frac{2r}{m}(\bar{u}))^{-7}$.

$$\nabla^2\bar{u} = \beta\left(1 - 7\alpha r\bar{u} + 28\alpha^2 r^2\bar{u}^2 - 84\alpha^3 r^3\bar{u}^3 + ...\right) \tag{2.5}$$

Where $\alpha = \frac{2}{m}$ and $\beta = -\frac{16r^7}{m^7}K_{ab}K^{ab}$. In this form we have the ability to take leading order approximations of this highly nonlinear equation in a much nicer looking arrangement. As we will soon see, we can easily locate the irregular terms by using this expansion and thus manage their impact on the numerical solver.

2.2 The Source Term

We define the source term to be the following component of the Hamiltonian, $-\frac{16r^7}{m^7}K_{ab}K^{ab}$, since all the components of the BHs spin and momentum are captured by this term. Solving the momentum constraint yields one possible solution for the extrinsic cur-

vature tensor. Although this solution is not unique, its simple form is appealing for the extensive calculations we will be performing with it. Here we have the following expression for the tensor,

$$K^{ab} = \frac{3}{2r^2}\left(P^a n_b + P^b n_a - (g^{ab} - n^a n^b)P^c n_c\right) + \frac{3}{r^3}\left(\epsilon^{acd} S_c n_d n^b + \epsilon^{bcd} S_c n_d n^a\right). \quad (2.6)$$

Where $n_a = \frac{x_a}{r}$ is the radial normal vector, $g_{ab} = \delta_{ab}$ the Kronecker Delta function, P^a is the a component of the BHs momentum vector, S^a is the a component of the BHs spin vector and ϵ^{abc} is an alternating tensor known as the Levi-Civita tensor that acts in the following way:

$$\epsilon_{abc} = \epsilon_{bca} = \epsilon_{cab} = 1$$

$$\epsilon_{acb} = \epsilon_{bac} = \epsilon_{cba} = -1$$

$$\epsilon_{aab} = \epsilon_{aca} = \epsilon_{bcc} = ... = 0 \text{ when indices are repeated}$$

The completely general source term with arbitrary spin and momentum vectors attains the following form

$$K_{ab}K^{ab} = \frac{9}{2r^4}(|\vec{P}|^2 + 2(\vec{P}\cdot\vec{n})^2) + \frac{18}{r^5}\vec{n}\cdot(\vec{P}\times\vec{S}) + \frac{18}{r^6}(|\vec{S}|^2 - (\vec{S}\cdot\vec{n})^2)$$

$$-\frac{16r^7}{m^7}K_{ab}K^{ab} = -\frac{72r^3}{m^7}(|\vec{P}|^2+2(\vec{P}\cdot\vec{n})^2) - \frac{288r^2}{m^7}\vec{n}\cdot(\vec{P}\times\vec{S}) - \frac{288r}{m^7}(|\vec{S}|^2-(\vec{S}\cdot\vec{n})^2) \quad (2.7)$$

Simplifications from this general case may be considered such as a BH with arbitrary spin and linear momentum in the z-direction. With these conditions the source term equates to

$$K_{ab}K^{ab} = 2\left[(1+2n_z^2)P_z^2\eta^2 - 2P_z\xi\eta(\vec{S}\times\vec{n})_z + \xi^2\left(\vec{S}^2 - (\vec{S}\cdot\vec{n})^2\right)\right]$$

where $\xi = 3/(r^3)$ and $\eta = 3/(2r^2)$.

We will be keeping with the fully arbitrary case for this paper to remain applicable to a BH with any variation of these parameters.

Expanding this equation out, we get the following expression:

$$K_{ab}K^{ab} = 2r^{-2}\Big[2\eta^2(P_x x + P_y y + P_z z)^2 + 2\xi\eta r\big((P_y S_z - P_z S_y)x + (P_z S_x - P_x S_z)y + (P_x S_y - P_y S_x)z\big) + \eta^2 r^2(P_x^2 + P_y^2 + P_z^2) + \xi^2\Big(r^2(S_x^2 + S_y^2 + S_z^2) - (S_x x + S_y y + S_z z)^2\Big)\Big].$$

Next we group the expression for $K_{ab}K^{ab}$ by powers of x, y and z. This form will be helpful when we introduce spherical harmonics into the equation.

$$\begin{aligned} K_{ab}K^{ab} = 2r^{-2}\Big[&(2P_x^2\eta^2 - \xi^2 S_x^2)x^2 + (2P_y^2\eta^2 - \xi^2 S_y^2)y^2 + (2P_z^2\eta^2 - \xi^2 S_z^2)z^2 \\ &+ 2\big(\eta^2 P_x P_y y + \xi\eta r(P_y S_z - P_z S_y) - \xi^2 S_x S_y y\big)x + 2\xi\eta r(P_z S_x - P_x S_z)y \\ &+ 2\big(\eta^2 P_y P_z y + \eta^2 P_x P_z x + \xi\eta r(P_x S_y - P_y S_x) - \xi^2 S_z(S_x x + S_y y)\big)z \\ &+ r^2\left(\eta^2(P_x^2 + P_y^2 + P_z^2) + \xi^2(S_x^2 + S_y^2 + S_z^2)\right)\Big]. \end{aligned} \tag{2.8}$$

Now we take our equation and put it into a form that will be useful later when we use spherical harmonics. We will use the fact that the following relationship holds

$$ax^2 + by^2 + cz^2 = \frac{a+b+c}{3}(x^2 + y^2 + z^2) + \frac{2c-a-b}{6}(2z^2 - x^2 - y^2) + \frac{a-b}{2}(x^2 - y^2)$$

where a, b, and c will be defined as the variable coefficients of x, y, and z respectively, from equation (3.8). Using these coefficients we can find the following quantities,

$$\begin{aligned} \frac{a+b+c}{3} &= \frac{2\left(2\eta^2(P_x^2 + P_y^2 + P_z^2) - \xi^2(S_x^2 + S_y^2 + S_z^2)\right)}{3} := \alpha_1 \\ \frac{2c-a-b}{6} &= \frac{2\left(2\eta^2(2P_z^2 - P_x^2 - P_y^2) - \xi^2(2S_x^2 - S_x^2 - S_y^2)\right)}{6} := \alpha_2 \\ \frac{a-b}{2} &= \frac{4\eta^2(P_x^2 - P_y^2) + 2\xi^2(S_y^2 - S_x^2)}{2} := \alpha_3 \end{aligned}$$

From here we can rewrite our source term from equation (3.8) with the use of spherical harmonics. We will come back to this after we define these harmonic modes and how

we will implement them.

2.3 Spherical Harmonics

Spherical harmonics are the angular component of the solution to Laplace's equation in spherical coordinates. The conversion from Cartesian coordinates to spherical coordinates follows these equations,

$$\begin{aligned} x &= r\sin(\theta)\cos(\phi) \\ y &= r\sin(\theta)\sin(\phi) \\ z &= r\cos(\theta) \end{aligned}$$

with the relationship, $\frac{x^2+y^2+z^2}{r^2} = 1$.

The notation for harmonic modes will be Y_{lm} and are represented by the following equation:

$$Y_{lm}(\theta,\phi) = Ne^{im\phi}P_{lm}(\cos\theta).$$

Here $P_{lm}(\cos\theta)$ is the associated Legendre Polynomial of degree l and order m. These modes form an orthogonal system which we will later use as a basis function to expand our $\bar{u}$ solution further, within the polynomial expansion.

Next we will re-normalize the harmonic modes to simplify the calculations in this paper and account for the normalization in the numerics. We only consider real-valued harmonic modes throughout this paper to simplify the numerical work. Since our code uses a spectral solver and does a good job of solving for coefficients, we have simplified the standard imaginary spherical harmonic table by the following method: If $m > 0$, then $Y_{lm} = Re[Y_{lm}]$ and if $m < 0$, then $Y_{lm} = -Im[Y_{lm}]$, usually taking the least common denominator as the coefficient.

For convenience and more symmetry later when we take products of modes, we will use the following normalization, breaking the rule that we usually go with the least common denominator integer coefficients on the following modes:

$$Y_{2,-2} = 2xy;\ Y_{3,-2} = 2xyz;\ Y_{4,-2} = 2xy(6z^2 - x^2 - y^2);\ Y_{4,-4} = 2xy(x^2 - y^2)$$

Thus, our complete list of redefined harmonic modes through fourth order appears as follows:

$$
\begin{aligned}
Y_{00} &= 1 \\
rY_{10} &= z \\
rY_{11} &= x \\
rY_{1,-1} &= y \\
r^2Y_{20} &= 2z^2 - x^2 - y^2 \\
r^2Y_{21} &= xz \\
r^2Y_{2,-1} &= yz \\
r^2Y_{22} &= x^2 - y^2 \\
r^2Y_{2,-2} &= 2xy \\
r^3Y_{30} &= 2z^3 - 3x^2z - 3y^2z \\
r^3Y_{31} &= 4xz^2 - x^3 - xy^2 \\
r^3Y_{3,-1} &= 4yz^2 - y^3 - x^2y \\
r^3Y_{32} &= (x^2 - y^2)z \\
r^3Y_{3,-2} &= 2xyz \\
r^3Y_{33} &= x^3 - 3xy^2 \\
r^3Y_{3,-3} &= 3x^2y - y^3 \\
r^4Y_{40} &= 3x^4 + 3y^4 + 8z^4 + 6x^2y^2 - 24x^2z^2 - 24y^2z^2 \\
r^4Y_{41} &= 4xz^3 - 3x^3z - 3xy^2z \\
r^4Y_{4,-1} &= 4yz^3 - 3y^3z - 3x^2yz \\
r^4Y_{42} &= y^4 - x^4 - 6y^2z^2 + 6x^2z^2 \\
r^4Y_{4,-2} &= 2xy(6z^2 - x^2 - y^2) \\
r^4Y_{43} &= x^3z - 3xy^2z \\
r^4Y_{4,-3} &= 3x^2yz - y^3z \\
r^4Y_{44} &= x^4 - 6x^2y^2 + y^4 \\
r^4Y_{4,-4} &= 2xy(x^2 - y^2)
\end{aligned}
$$

Using these harmonic modes, we return to pick up where we left off with the source term.

In two steps we will replace all of the Cartesian position coordinates with harmonic modes. The first step is a rearrangement to fit the form of the modes in a way that the second step is a simple substitution using the definitions above.

$$K_{ab}K^{ab} = \left(\alpha_1 + 2(\eta^2\vec{P}^2 + \xi^2\vec{S}^2)\right)Y_{00} + \alpha_2 Y_{20} + \alpha_3 Y_{22} + 4\eta\xi(P_xS_y - P_yS_x)\frac{z}{r} + 4\eta\xi(P_yS_z - P_zS_y)\frac{x}{r} + 4\eta\xi(P_zS_x - P_xS_z)\frac{y}{r} + 4(2\eta^2P_xP_y - \xi^2S_xS_y)\frac{xy}{r^2} + 4(2\eta^2P_xP_z - \xi^2S_xS_z)\frac{xz}{r^2} + 4(2\eta^2P_yP_z - \xi^2S_yS_z)\frac{yz}{r^2}.$$

$$K_{ab}K^{ab} = \left(\alpha_1 + 2(\eta^2\vec{P}^2 + \xi^2\vec{S}^2)\right)Y_{00} + \alpha_2 Y_{20} + \alpha_3 Y_{22} + 4\eta\xi(P_xS_y - P_yS_x)Y_{10} + 4\eta\xi(P_yS_z - P_zS_y)Y_{11} + 4\eta\xi(P_zS_x - P_xS_z)Y_{1,-1} + 4(2\eta^2P_xP_y - \xi^2S_xS_y)Y_{2,-2} + 4(2\eta^2P_xP_z - \xi^2S_xS_z)Y_{21} + 4(2\eta^2P_yP_z - \xi^2S_yS_z)Y_{2,-1}. \quad (2.9)$$

where α_1, α_2 and α_3 are defined earlier.

This is a very critical expression, representing the extrinsic curvature of our black hole with arbitrary spin and momentum written in terms of spherical harmonics. Looking back at our expansion from EQ (2.5), the full first term in that series is the source term, β, which is simply EQ (2.9) multiplied by a factor of $\frac{-16r^7}{m^7}$.

We now have all the pieces in place that we will use to manipulate the Hamiltonian constraint into a form that we can use to resolve our numerical issues. In the next chapter we will explicitly merge the polynomial expansion with the harmonic expansion in order to numerically solve the Hamiltonian more efficiently by recovering *irregular* components from these expansions. The use of these and other expansions will allow us to locate the irregularities present in a straight forward manor.

Harmonic Plots

In order to get more acquainted with spherical harmonics and some of their properties, below are plots representing these functions up through third order in l. If we plot the magnitude squared of the harmonic functions then we can see how they make an excellent candidate for a basis in a spherical system. In the following plots we can see how they partition and spherical coordinate system at the poles and equatorial region in

a very interesting way. The plots consider the modulus squared of the full complex mode along with the real and imaginary distinction. The real and imaginary components of the modes correspond to the $\pm m$ values respectively. The negative order harmonics $Y_{l,-m}$ are rotated about the z axis by $90°/m$ with respect to the positive order ones, making the $-m$-modes a rotation out of phase with their positive counterpart.

The arrangement of the plots will be such that Y_{00} appears first and alone, while the next orders of l get their own page, and for $l = 3$ we have broken that order up to fit on two pages.

Y_{00} Mode

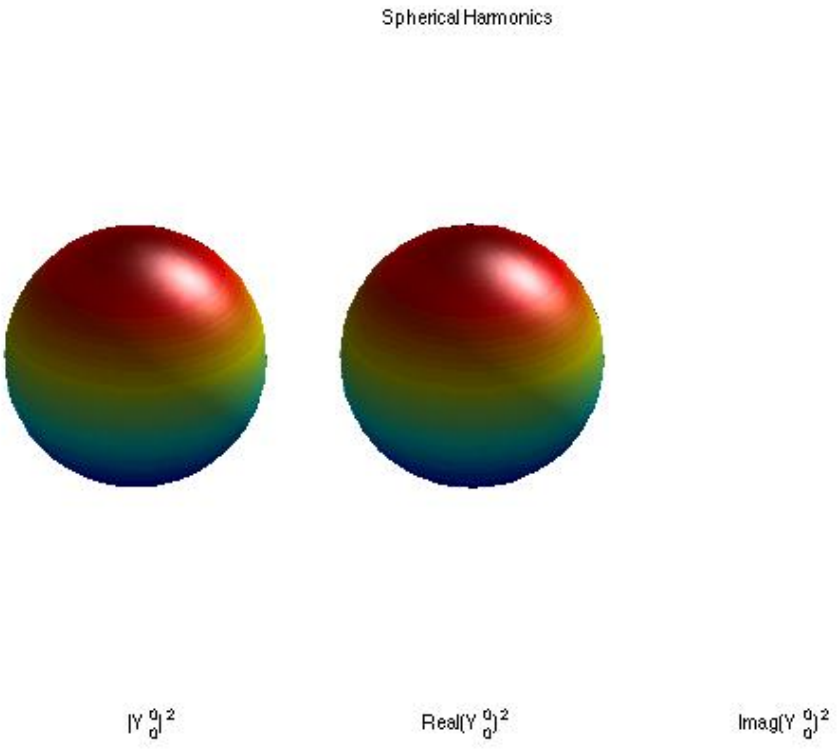

Figure 2.1: Y_{00} Mode

Y_{1m} Modes

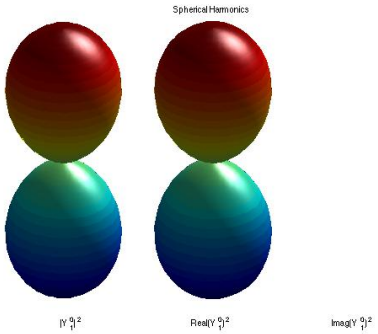

Figure 2.2: Y_{10} Mode

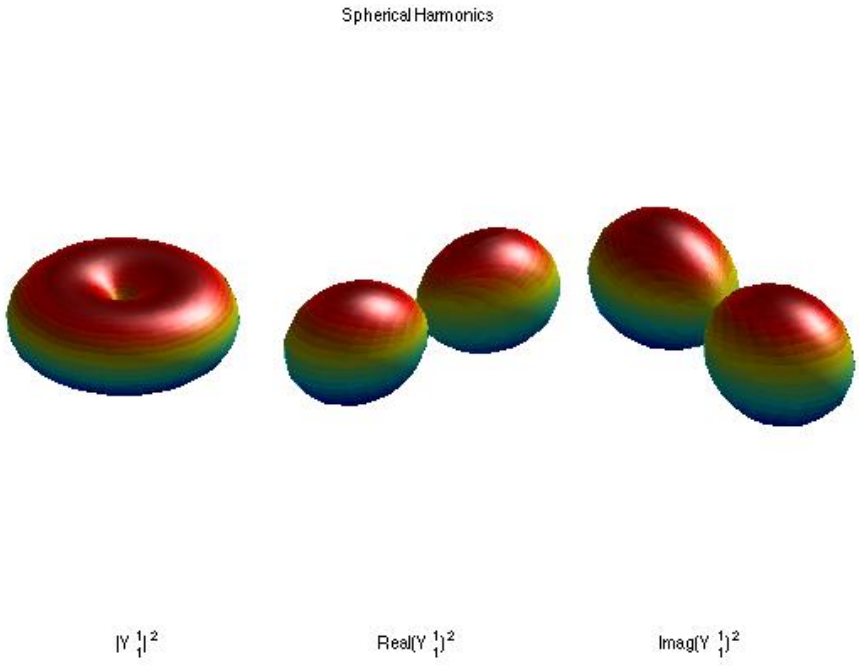

Figure 2.3: Y_{11} & $Y_{1,-1}$ Modes

Y_{2m} Modes

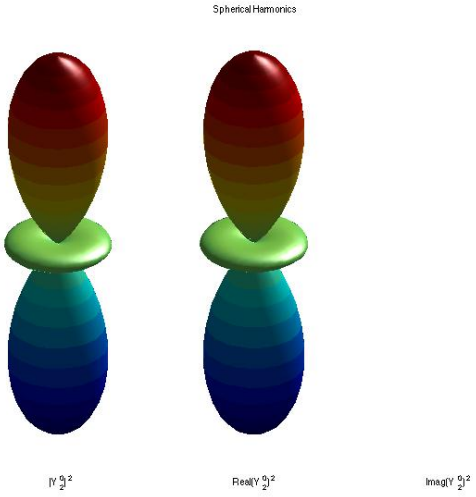

Figure 2.4: Y_{20} Mode

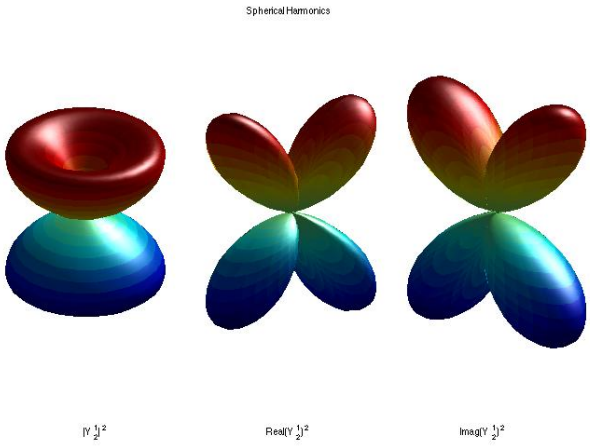

Figure 2.5: Y_{21} & $Y_{2,-1}$ Modes

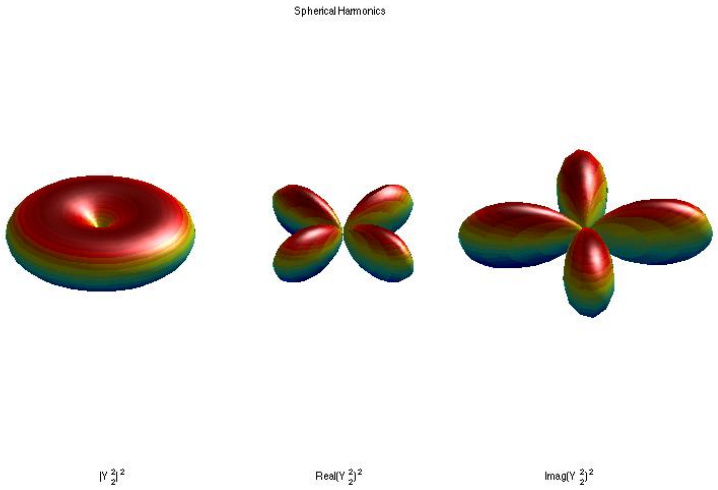

Figure 2.6: Y_{22} & $Y_{2,-2}$ Modes

Y_{3m} Modes

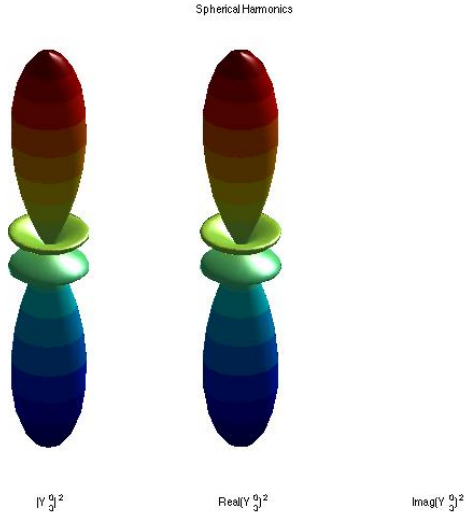

Figure 2.7: Y_{30} Mode

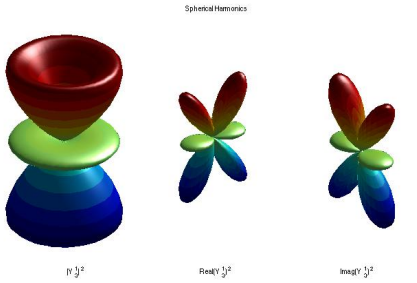

Figure 2.8: Y_{31} & $Y_{3,-1}$ Modes

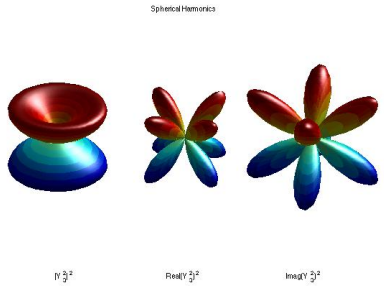

Figure 2.9: Y_{32} & $Y_{3,-2}$ Modes

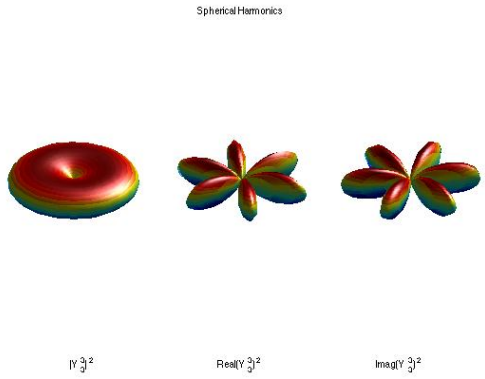

Figure 2.10: Y_{33} & $Y_{3,-3}$ Modes

Chapter 3

Using the Polynomial Expansion

Now that we have an understanding of spherical harmonics we can combine this idea with the polynomial expansion to rewrite the Hamiltonian in terms of these harmonic modes. As we will see, doing this makes classification of regular and irregular terms very straight forward. We will be able to identify these terms simply by looking at the parity between the harmonic mode l component and the power of r associated with the term. The nonlinear nature of the Hamiltonian combined with the lengthy expressions of the source term, and others to come, make the task of achieving a fourth order approximation nontrivial and requires detailed tracking methods for all the elements involved. We start this chapter by outlining more of the infrastructure we used to locate the irregularities and conclude with both the full regular and irregular components of the Hamiltonian, up through fourth order, represented in a way that can be solved by standard methods.

3.1 Expanding the Expansion

We are already familiar with the polynomial expansion around the scalar field substituted variable $\bar{u}$, which reads as follows:

$$\nabla^2 \bar{u} = -\frac{16r^7}{m^7} K_{ab}K^{ab}\left(1 - 7\alpha r\bar{u} + 28\alpha^2 r^2\bar{u}^2 - 84\alpha^3 r^3\bar{u}^3 + ...\right) \tag{3.1}$$

Where $\alpha = \frac{2}{m}$.

This expansion, however, only gets us partially to the point where we can fully resolve the inherent issues of regularity. The reason for this is found in the nonlinear character on the right hand side. Irregularities are a natural part of this equation, and thus the solution. In order to fully account for these problematic pieces, we expand our $\bar{u}$-solution in the following way,

$$\bar{u} = H(\bar{u}(r)) + R(\bar{u}(r)) + I(\bar{u}(r)). \tag{3.2}$$

By splitting our solution into regular, irregular and homogeneous, $(R, I\&H)$, components we fully accounts for the solution and allows us a nice way to properly deal with irregularities introduced through $\bar{u}$. Regular terms are terms in which the parity between the harmonic modes and power of r are both even or odd. The homogeneous portion accounts for the homogeneous solutions and are determined numerically.

The first term in EQ 3.1 does not contain any nonlinear contribution. Multiplying this term out fully, we have

$$\begin{aligned}
\nabla^2\bar{u} \;\approx\; & \frac{-1}{m^7}\Big[24r^3\Big(5Y_{00}(P_x^2+P_y^2+P_z^2) + Y_{20}(2P_z^2-P_x^2-P_y^2) + 12Y_{21}P_xP_z \\
& + 12Y_{2,-1}P_yP_z + 3Y_{22}(P_x^2-P_y^2) + 12Y_{2,-2}P_xP_y\Big) \\
& + 288r^2\Big(Y_{10}(P_xS_y - P_yS_x) + Y_{11}(P_yS_z - P_zS_y) + Y_{1,-1}(P_zS_x - P_xS_z)\Big) \\
& + 48r\Big(4Y_{00}(S_x^2+S_y^2+S_z^2) + Y_{20}(S_x^2+S_y^2-2S_z^2) + 3Y_{22}(S_y^2-S_x^2) \\
& - 12Y_{2,-2}(S_xS_y) - 12Y_{21}(S_xS_z) - 12Y_{2,-1}(S_yS_z)\Big)\Big].
\end{aligned} \tag{3.3}$$

This is the full source term for one BH with arbitrary spin and momentum represented with spherical harmonics. This will be a key component in our classification scheme and it also depicts the length scale of the equation we are working with, as this is just the first term multiplied out and doesn't involve $\bar{u}$. Within this term is the full first order approximation, as well as part of the second and third orders since more terms appear for these orders when we multiply EQ 3.1 out further. Since we are striving for a fourth order approximation, we will need the proceeding multiplication steps from EQ 3.1, which all involve powers of $\bar{u}$. In order to gain a fourth order approximation, we will carefully treat the powers of $\bar{u}$ with the expression from EQ 3.2.

3.2 Finding the Irregular Terms

Finding the irregularities in our equation is essential to improving our numerical data modeling the BH. As mentioned, we can identify the irregular terms by looking at the powers of are that are offset with the $l-$component of the harmonic modes, in an even/odd sense. Looking back at our source term, $\frac{-16r^7}{m^7}K_{ij}K^{ij}$, every component has this mode discrepancy with powers of r, r^2 and r^3. Since, in the polynomial expansion, we multiply the source term with increasing powers of r and also with varying harmonic modes, the regularity of a given component is effected when multiplied with combinations of those two factors.

To help us identify irregularities and manage these lengthy lists of figures, we restructure our equation to both simplify the RHS and portray the necessary information needed to locate these irregular components. First, we take the source term from EQ 3.3 and represent it in a summation form over the harmonic modes:

$$-\frac{16r^7}{m^7}K_{ab}K^{ab} = \sum_{l,m}^{\infty}\alpha_{lm}rY_{lm} + \sum_{m}^{\infty}\beta_m r^2 Y_{1m} + \sum_{l,m}^{\infty}\gamma_{lm}r^3Y_{lm}. \tag{3.4}$$

Here we have captured the full content of the source term in three compact summations where the constants $\alpha_{lm},\ \beta_m$, and γ_{lm} are the pure spin term, the spin momentum cross term and the pure momentum term, respectively. Expanded back out in this grouping, we have

$$\alpha_{l,m} = -\frac{48}{m^7}\begin{cases} 4(S_x^2+S_y^2+S_z^2); & l,m=0,0 \\ S_x^2+S_y^2-2S_z^2; & l,m=2,0 \\ -12S_xS_z; & l,m=2,1 \\ -12S_yS_z; & l,m=2,-1 \\ 3(-S_x^2+S_y^2); & l,m=2,2 \\ -12S_xS_y; & l,m=2,-2 \end{cases}$$

$$\beta_m = -\frac{288}{m^7}\begin{cases} P_xS_y - P_yS_x; & l,m = 1,0 \\ P_yS_z - P_zS_y; & l,m = 1,1 \\ P_zS_x - P_xS_z; & l,m = 1,-1 \end{cases}$$

$$\gamma_{lm} = -\frac{24}{m^7}\begin{cases} 5(P_x^2 + P_y^2 + P_z^2); & l,m = 0,0 \\ 2P_z^2 - P_x^2 - P_y^2; & l,m = 2,0 \\ 12P_xP_z; & l,m = 2,1 \\ 12P_yP_z; & l,m = 2,-1 \\ 3(P_x^2 - P_y^2); & l,m = 2,2 \\ 12P_xP_y; & l,m = 2,-2 \end{cases}$$

Applying this same idea to the $\bar{u}$ expression from EQ 3.2, we call on the orthogonality of the spherical harmonic modes to expand $\bar{u}$ it with them as basis functions and represent our solution as the following:

$$\bar{u} = \sum_{n=0}^{\infty}\sum_{l,m} H_{nlm}r^nY_{l,m} + \sum_{n=3}^{\infty}\sum_{l,m} I_{nlm}r^nY_{l,m} + \sum_{n=4}^{\infty}\sum_{l,m} R_{nlm}r^nY_{l,m}. \tag{3.5}$$

where H_{nlm}, R_{nlm} and I_{nlm} are coefficients for the homogeneous, regular and irregular components of $\bar{u}$, respectively.

Note that the initial powers of r in each summation vary in EQ 3.5. Since solving for $\bar{u}$ requires an inverse Laplace operation, which raises the power of r by 2, the resulting lowest order behavior of $\bar{u}$ comes from the first irregular term starting at an order of r^1. Likewise the first regular term has power r^2 as the lowest order and thus an inverse Laplace operation would result with an r^4 term. The homogeneous portion of $\bar{u}$ is derived numerically and will account for constant pieces as well as r dependence.

By combining EQs 3.4 & 3.5 in the following way, we can begin our classification.

$$\nabla^2\bar{u} = \left[\sum_{l,m}^{\infty}\alpha_{lm}rY_{lm} + \sum_{m}^{\infty}\beta_m r^2 Y_{1m} + \sum_{l,m}^{\infty}\gamma_{lm}r^3Y_{lm}\right] \\ \text{X}\left(1 - \frac{14r}{m}\bar{u} + \frac{56r^2}{m^2}(\bar{u}^2) - \frac{672r^3}{m^3}(\bar{u}^3) + ...\right) \tag{3.6}$$

Once we have this equation, finding the irregular terms may be identified with ease. To present this combination more clearly, we suppress the last expansion of $\bar{u}$ from EQ 3.5, but will keep it in mind for what follows.

A categorical representation of this multiplication and classification will be presented in Table 3.1 and described throughout the rest of this chapter. The nonlinear character of the Hamiltonian starts to effect our polynomial expansion at order r^2. This is due to the homogeneous contribution from the $\bar{u}$-solution in the polynomial expansion multiplied with the pure spin element of the source term.

Now, under the mode definitions defined in the previous chapter, we may work out some products that will be needed in to identify irregularities. The following quantities are useful for finding the mode product representations:

$$\begin{aligned} z^2 &= \frac{1}{3}r^2(Y_{00} + Y_{20}) \\ x^2 + y^2 = r^2 - z^2 &= \frac{1}{3}r^2(2Y_{00} - Y_{20}) \\ x^2 &= \frac{1}{6}r^2(2Y_{00} - Y_{20} + 3Y_{22}) \\ y^2 + z^2 = r^2 - x^2 &= \frac{1}{6}r^2(4Y_{00} + Y_{20} - 3Y_{22}) \\ y^2 &= \frac{1}{6}r^2(2Y_{00} - Y_{20} - 3Y_{22}) \\ x^2 + z^2 = r^2 - y^2 &= \frac{1}{6}r^2(4Y_{00} + Y_{20} + 3Y_{22}) \end{aligned}$$

For the purpose of identifying irregular terms and implementing the mathematics in our code, we define any mode product as the sum of other known modes. This results in unique representations of the products and yields the mode parity information we need in classifying. Bellow we have a list of all possible products through fourth order.

$$
\begin{aligned}
Y_{11}Y_{11} &= x^2 = & \frac{1}{6}(3Y_{22} - Y_{20} + 2Y_{00}) \\
Y_{10}Y_{10} &= z^2 = & \frac{1}{3}(Y_{20} + Y_{00}) \\
Y_{1,-1}Y_{1,-1} &= y^2 = & \frac{1}{6}(-3Y_{22} - Y_{20} + 2Y_{00}) \\
Y_{11}Y_{10} &= xz = & Y_{21} \\
Y_{11}Y_{1,-1} &= xy = & \frac{Y_{2,-2}}{2} \\
Y_{10}Y_{1,-1} &= yz = & Y_{2,-1}
\end{aligned}
$$

$$
\begin{aligned}
Y_{11}Y_{00} &= x = & Y_{11} \\
Y_{11}Y_{22} &= x(x^2 - y^2) = x^3 - xy^2 = & \frac{1}{10}\left(5Y_{33} - Y_{31} + 4Y_{11}\right) \\
Y_{11}Y_{21} &= x(xz) = x^2 z = & \frac{1}{10}\left(5Y_{32} - Y_{30} + 2Y_{10}\right) \\
Y_{11}Y_{20} &= x(2z^2 - x^2 - y^2) = -x^3 - xy^2 + 2xz^2 = & \frac{1}{5}\left(3Y_{31} - 2Y_{11}\right) \\
Y_{11}Y_{2,-1} &= x(yz) = xyz = & \frac{1}{2}Y_{3,-2} \\
Y_{11}Y_{2,-2} &= x(2xy) = 2x^2 y = & \frac{1}{10}\left(5Y_{3,-3} - Y_{3,-1} + 4Y_{1,-1}\right)
\end{aligned}
$$

$$
\begin{aligned}
Y_{10}Y_{00} &= z = & Y_{10} \\
Y_{10}Y_{22} &= z(x^2 - y^2) = x^2 z - y^2 z = & Y_{32} \\
Y_{10}Y_{21} &= z(xz) = xz^2 = & \frac{1}{5}\left(Y_{31} + Y_{11}\right) \\
Y_{10}Y_{20} &= z(2z^2 - x^2 - y^2) = -x^2 z - y^2 z + 2z^3 = & \frac{1}{5}\left(3Y_{30} + 4Y_{10}\right) \\
Y_{10}Y_{2,-1} &= z(yz) = yz^2 = & \frac{1}{5}\left(Y_{3,-1} + Y_{1,-1}\right) \\
Y_{10}Y_{2,-2} &= z(2xy) = 2xyz = & Y_{3,-2}
\end{aligned}
$$

$$
\begin{aligned}
Y_{1,-1}Y_{00} &= y = & Y_{1,-1} \\
Y_{1,-1}Y_{22} &= y(x^2-y^2) = x^2y - y^3 = & \frac{1}{10}\left(5Y_{3,-3} + Y_{3,-1} - 4Y_{1,-1}\right) \\
Y_{1,-1}Y_{21} &= y(xz) = xyz = & \frac{1}{2}Y_{3,-2} \\
Y_{1,-1}Y_{20} &= y(2z^2-x^2-y^2) = -x^2y - y^3 + 2yz^2 = & \frac{1}{5}\left(3Y_{3,-1} - 2Y_{1,-1}\right) \\
Y_{1,-1}Y_{2,-1} &= y(yz) = y^2z = & \frac{1}{10}\left(-5Y_{32} - Y_{30} + 2Y_{10}\right) \\
Y_{1,-1}Y_{2,-2} &= y(2xy) = 2xy^2 = & \frac{1}{10}\left(-5Y_{33} - Y_{31} + 4Y_{11}\right)
\end{aligned}
$$

$$
\begin{aligned}
Y_{22}Y_{22} &= \frac{1}{210}(105Y_{44} + 3Y_{40} - 40Y_{20} + 56Y_{00}) \\
Y_{21}Y_{21} &= \frac{1}{210}(15Y_{42} - 3Y_{40} + 15Y_{22} + 5Y_{20} + 14Y_{00}) \\
Y_{20}Y_{20} &= \frac{1}{35}(9Y_{40} + 20Y_{20} + 28Y_{00}) \\
Y_{2,-1}Y_{2,-1} &= \frac{1}{210}(-15Y_{42} - 3Y_{40} - 15Y_{22} + 5Y_{20} + 14Y_{00}) \\
Y_{2,-2}Y_{2,-2} &= \frac{1}{210}(-105Y_{44} + 3Y_{40} - 40Y_{20} + 56Y_{00})
\end{aligned}
$$

$$
Y_{22}Y_{2,-2} = Y_{4,-4}
$$

$$
\begin{aligned}
Y_{22}Y_{21} &= \frac{1}{14}(7Y_{43} - Y_{41} + 4Y_{21}) \\
Y_{2,-2}Y_{2,-1} &= \frac{1}{14}(-7Y_{43} - Y_{41} + 4Y_{21}) \\
Y_{22}Y_{2,-1} &= \frac{1}{14}(7Y_{4,-3} + Y_{4,-1} - 4Y_{2,-1}) \\
Y_{2,-2}Y_{21} &= \frac{1}{14}(7Y_{4,-3} - Y_{4,-1} + 4Y_{2,-1})
\end{aligned}
$$

$$
\begin{aligned}
Y_{22}Y_{20} &= \frac{1}{7}(3Y_{42} - 4Y_{22}) \\
Y_{2,-2}Y_{20} &= \frac{1}{7}(3Y_{4,-2} - 4Y_{2,-2})
\end{aligned}
$$

$$
\begin{aligned}
Y_{21}Y_{20} &= \frac{1}{7}(3Y_{41} + 2Y_{21}) \\
Y_{2,-1}Y_{20} &= \frac{1}{7}(3Y_{4,-1} + 2Y_{2,-1}) \\
Y_{21}Y_{2,-1} &= \frac{1}{14}(Y_{4,-2} + Y_{2,-2})
\end{aligned}
$$

Using these products with EQ 3.6, we may now easily pick out the irregular components by stepping through the multiplication in EQ 3.6 term by term. There are a couple important elements to keep track of while we are classifying these products: the powers of r from the Taylor expansion, the harmonic mode products between the source term and portions of $\bar{u}$, and nonlinear contributions in the form of homogeneous coefficients and powers of r the come from the solution.

Table 3.1 contains the terms from the polynomial expansion and their classification as either regular or irregular, which is based on the even-odd parity described earlier after taking all products from EQ 3.6 up through fourth order. Noticing the pattern developed by Table 3.1, we can postulate that fifth order will have mostly irregular terms, as well as contributions from the irregular coefficients described by EQ 3.5, which we are avoiding in this paper. In order to condense large expressions in Table 3.1, we use the α, β, γ notation from EQ 3.4.

Generating this list makes it clear why we would want to try handling the irregular characteristics of the Hamiltonian in a more effective way since they have a large influence in the first four orders of r.

Table 3.1: Regular and Irregular Classification of $\nabla^2\bar{u}$ through Fourth Order in r

Powers of r	Regular	Irregular
1		$\sum \alpha_{lm}Y_{lm}$
2	$\frac{-14}{m}\sum \alpha_{lm}Y_{lm}H_{000}$	$\sum \beta_m Y_{1m}$
3	$\sum \beta_m Y_{1m}H_{000}$	$\sum \gamma_{lm}Y_{lm}$
	$\frac{-14}{m}\sum \alpha_{lm}Y_{lm}\sum_M H_{11M}Y_{1M}$	$\frac{56}{m^2}\sum \alpha_{lm}Y_{lm}(H_{000})^2$
4	$\frac{-14}{m}\sum \alpha_{lm}Y_{lm}\sum H_{2lm}Y_{lm}$	$\frac{56}{m^2}\sum \beta_m Y_{1m}(H_{000})^2$
	$\frac{-672}{m^3}\sum \alpha_{lm}Y_{lm}(H_{000})^3$	$\frac{56}{m^2}\sum \alpha_{lm}Y_{lm}\sum_M 2H_{000}H_{11M}Y_{1M}$
	$\frac{-14}{m}\sum \beta_m Y_{1m}\sum_M H_{11M}Y_{1M}$	
	$\frac{-14}{m}\sum \gamma_{lm}Y_{lm}H_{000}$	

3.3 Full Fourth Order Irregularity

Attaining the full analytic representation for the irregular component of the Hamiltonian, up through fourth order, is necessary for our numerical scheme. In this section we explicitly show how the full irregular term was found and write out exactly what we will need to solve and code it.

The expansion of $\bar{u}$ in different source modes described by EQ 3.5 contains all the terms we are trying to identify, namely the middle summation representing the irregular component of the solution. Again, irregular terms are identified based on the values of n and l having opposite even/odd parities. For every case described in this paper, we note that $n \geq |l|$, i.e. we have no modes present in the solution that are not at least continuous.

From EQ 3.5, we see $\bar{u}$ is solely represented by homogeneous terms up to second order

in r, thus $r\bar{u}$ contains just homogeneous contributions up to third-order and the RHS of the Laplacian up to fourth order. If we truncate our expansion there, we need not consider non-linear effects from either the irregular or regular inhomogeneous terms appearing on the RHS of the Hamiltonian, making a fourth order bench mark a good candidate. Using the expansions for $\bar{u}$ from EQ 3.5, the truncation of $\bar{u}$'s nonlinear contributions from the polynomial expansion up to third order in r are the following terms:

$$r\bar{u} = H_{000}r + \sum_m H_{11m}Y_{1m}r^2 + H^+_{22m}Y^+_{2m}r^3 \tag{3.7a}$$

$$(r\bar{u})^2 = (H_{000})^2r^2 + 2\sum_m H_{000}H_{11m}Y_{1m}r^3 \tag{3.7b}$$

$$(r\bar{u})^3 = (H_{000})^3r^3 \tag{3.7c}$$

Where the term $H^+_{22m}Y^+_{2m}r^3$ includes the Y_{00} mode as well. For the rest of this chapter, Y^+_{lm} incidactes the inclusion of Y_{00} in the expression.

The terms at order r^1 and r^2 are the $K_{ij}K^{ij}$ source components we have seen before. At r^3 we start to get more interesting terms that display the nonlinear aspect of the Hamiltonian with the introduction of H_{000}. Using the truncation from EQs 3.7a-c, we may rewrite EQ 3.6 with $\bar{u}$ replaced by it's homogeneous components.

$$\begin{aligned}\nabla^2\bar{u} = &\left[\sum_{l,m}^{\infty}\alpha_{lm}rY_{lm} + \sum_m^{\infty}\beta_m r^2Y_{1m} + \sum_{l,m}^{\infty}\gamma_{lm}r^3Y_{lm}\right] \\ &\text{X}\left[1 - 7\kappa\left(H_{000}r + \sum_m H_{11m}Y_{1m}r^2 + H^+_{22m}Y^+_{2m}r^3\right)\right. \\ &\left. + 28\kappa^2\left((H_{000})^2r^2 + 2\sum_m H_{000}H_{11m}Y_{1m}r^3\right) - 84\kappa^3(H_{000}r)^3 + ...\right]\end{aligned} \tag{3.8}$$

where $\kappa = \frac{2}{m}$.

Now, since $\bar{u}$ is regular up to third order, it follows that $r\bar{u}$ and $(r\bar{u})^3$ are irregular up to third order, while $(r\bar{u})^2$ is regular. When we multiply by the spin and momentum-related components of the source term, which are irregular, we find our only irregular contributions arise either from the original factor of unity or the $(r\bar{u})^2$ term.

Thus, up to fourth-order in r, our irregular source terms take the following form:

$$\nabla^2 \bar{u}^{irreg} = r\left[\sum_m \alpha_m^+ Y_{2m}^+\right] + r^2\left[\sum_m \beta_m Y_{1m}\right] + r^3\left[\sum_m \left(\gamma_m^+ + (H_{000})^2\alpha_m^+\right) Y_{2m}^+\right] + r^4\left[(H_{000}^2)\sum_m \beta_m Y_{1m} + 2H_{000}\sum_m\sum_M H_{11m}\alpha_{2M}^+ Y_{1m}Y_{2M}^+\right] + ... \quad (3.9)$$

The constants from the Taylor expansion have been absorbed into the sum.

There is only one irregular term involving mode products on the RHS. In order to use this in our code we expanded this term based on the products defined above.

$$RHS_{irreg} = 56r^4\kappa^2 H_0 \sum_m\sum_M H_{1m}\alpha_m^+ Y_{1m}Y_{2M}^+ \quad (3.10)$$

$$= 56r^4\kappa^2 H_0 \left[\begin{array}{l} \frac{1}{5}Y_{11}\left\{H_{1x}(5\alpha_{00}+2\alpha_{22}-2\alpha_{20}) + H_{1z}\alpha_{21} + 2H_{1y}\alpha_{2,-2}\right\} \\ +\frac{1}{5}Y_{10}\left\{H_{1x}\alpha_{21} + H_{1z}(5\alpha_{00}+4\alpha_{20}) + H_{1y}\alpha_{2,-1}\right\} \\ +\frac{1}{5}Y_{1,-1}\left\{2H_{1x}\alpha_{2,-2} + H_{1z}\alpha_{2,-1} + H_{1y}(5\alpha_{00}-2\alpha_{22}-2\alpha_{20})\right\} \\ +\frac{1}{2}Y_{33}\{H_{1x}\alpha_{22} - H_{1y}\alpha_{2,-2}\} \\ +\frac{1}{2}Y_{32}\{H_{1x}\alpha_{21} + 2H_{1z}\alpha_{22} - H_{1y}\alpha_{2,-1}\} \\ +\frac{1}{10}Y_{31}\{H_{1x}(-\alpha_{22}+6\alpha_{20}) + 2H_{1z}\alpha_{21} - H_{1y}\alpha_{2,-2}\} \\ +\frac{1}{10}Y_{30}\{-H_{1x}\alpha_{21} + 6H_{1z}\alpha_{20} - H_{1y}\alpha_{2,-1}\} \\ +\frac{1}{10}Y_{3,-1}\{-H_{1x}\alpha_{2,-2} + 2H_{1z}\alpha_{2,-1} + H_{1y}(\alpha_{22}+6\alpha_{20})\} \\ +\frac{1}{2}Y_{3,-2}\{H_{1x}\alpha_{2,-1} + 2H_{1z}\alpha_{2,-2} + H_{1y}\alpha_{21}\} \\ +\frac{1}{2}Y_{3,-3}\{H_{1x}\alpha_{2,-2} + H_{1y}\alpha_{22}\} \end{array}\right]$$

In the next section we will see how we can solve for $\bar{u}^{irreg}$ up through fourth order by performing an inverse Laplace operation on EQ 3.9. Doing this allows us to remove

a large part of the Hamiltonian from a numerical method, which would improperly handle the entire term, by subtracting it out during the solving process and adding it back fully solved after the fact.

3.4 The Inverse Laplacian

Now that we have captured all the elements of the Hamiltonian up to fifth order, and separated out the ones that cause the issues in our numerical scheme, we will now solve for these irregularities explicitly by taking the inverse Laplacian across each term. Having the Hamiltonian represented as sums of terms that have the form Cr^nY_{lm}, where $C \epsilon \mathbb{R}$, is a huge advantage when performing this operation, since inverting the Laplacian is a linear operation. First we will prove how the inverse Laplacian acts on a function like ours and then use it to resolve the irregular terms for use in our numerical process.

For any function expanded in powers of r and angular spherical harmonics, the inverse Laplacian may be written down explicitly. The following equations were both derived from Laplace's equation in spherical coordinates.

$$\Delta r^n Y_{lm} = \nabla^2 r^n Y_{lm} = [n(n+1) - l(l+1)] r^{n-2} Y_{lm}. \tag{3.11}$$

Then from here we find the inverse operation to be:

$$\Delta^{-1} r^n Y_{lm} = \frac{r^{n+2} Y_{lm}}{(n+2)(n+3) - l(l+1)}. \tag{3.12}$$

Proof:

It can be derived from Laplace's equation in spherical coordinates that the harmonic Y_{lm} modes are eigenfunctions that satisfy

$$r^2 \Delta Y_{lm} = -l(l+1) Y_{lm}.$$

From here we use the definition of the Laplacian in spherical coordinates on $\Delta r^n Y_{lm}$

$$\Delta r^n Y_{lm} = \frac{1}{r^2}\frac{\partial}{\partial r}\left(r^2\frac{\partial r^n Y_{lm}}{\partial r}\right) + \frac{1}{r^2\sin(\theta)}\frac{\partial}{\partial\theta}\left(\sin(\theta)\frac{\partial r^n Y_{lm}}{\partial\theta}\right) + \frac{1}{r^2\sin^2(\theta)}\frac{\partial^2 r^n Y_{lm}}{\partial\phi^2}$$

Since the harmonic modes are independent of r, the proof follows very straight forwardly,

$$\begin{aligned}\Delta r^n Y_{lm} &= \frac{1}{r^2}\frac{\partial}{\partial r}\left(nr^{n+1}Y_{lm}\right) + r^n(\Delta Y_{lm}) \\ \Delta r^n Y_{lm} &= n(n+1)r^{n-2}Y_{lm} + r^n(\Delta Y_{lm})\end{aligned}$$

From here we use the definition of the Laplacian for Y_{lm} to reach our result

$$\begin{aligned}\Delta r^n Y_{lm} &= n(n+1)r^{n-2}Y_{lm} + r^n(-l(l+1)r^{-2}Y_{lm}) \\ &= [n(n+1) - l(l+1)]r^{n-2}Y_{lm}\ \square\end{aligned}$$

To prove the definition of the inverse Laplacian we simply apply the Laplacian to the inverse and regain $r^n Y_{lm}$ as a result.

$$\begin{aligned}\Delta^{-1}\left(\Delta r^n Y_{lm}\right) &= [n(n+1) - l(l+1)]\Delta^{-1}\left(r^{n-2}Y_{lm}\right) \\ r^n Y_{lm} &= [n(n+1) - l(l+1)]\frac{r^n Y_{lm}}{n(n+1) - l(l+1)} \\ &= r^n Y_{lm}\end{aligned}$$

The result also holds when the inverse commutes with the Laplace operator. As we will see, this operator is significant since it allows us a straight forward way to solve for and subtract out any part of the equation we choose. With this we will solve for both the regular and irregular terms through fourth order. We solve for the regular terms as well to show that our representations of the Hamiltonian are indeed accurate up to fourth order by subtracting off both the regular and irregular terms.

3.5 Testing Validity

Using the regularity break down we have outlined, we can test the full fourth order approximation against the pseudo spectral code. By taking the difference between the

full fourth order approximation and the original pseudo spectral code we expect the resulting data to have r^5 behavior as this will be leading order. Below we full classify the regular component of the Hamiltonian up to fifth order and show the aforementioned subtraction will reflect a fifth order convergence.

There are three regular terms that are nontrivial and involve mode products. The first one of these terms comes in at r^3 as the following:

$$-7\kappa r^3 \sum_m \sum_M H_{1m}\alpha_m^+ Y_{1m} Y_{2M}^+ = -7\kappa r^3 \left[...\right]$$

with the term in brackets having the same elements from the brackets in EQ 3.10. The other two terms come in at fourth order:

$$RHS_{reg;1} = -7\kappa r^4 \sum_m \sum_M H_{1m}\beta_M Y_{1m} Y_{1M}$$

$$= -7\kappa r^4 \left[\begin{array}{l} \frac{1}{3}Y_{00}(H_{1x}\beta_1 + H_{1z}\beta_0 + H_{1y}\beta_{-1}) \\ \\ +\frac{1}{2}Y_{22}(H_{1x}\beta_1 - H_{1y}\beta_{-1}) + \frac{1}{6}Y_{20}(-H_{1x}\beta_1 + 2H_{1z}\beta_0 - H_{1y}\beta_{-1}) \\ \\ +Y_{21}(H_{1x}\beta_0 + H_{1z}\beta_1) + Y_{2,-1}(H_{1z}\beta_{-1} + H_{1y}\beta_0) + \frac{1}{2}Y_{2,-2}(H_{1x}\beta_{-1} + H_{1y}\beta_1) \end{array} \right]$$

The latter is longer, and please note that $H_{00}^+ \neq H_{00}$, as the former is the r^2 isotropic (traceless) behavior of the homogeneous solution. We only use it in the expression below:

$$RHS_{reg;2} = -7\kappa r^4 \sum_m \sum_M H_{2m}^+ \alpha_M^+ Y_{2m}^+ Y_{2M}^+$$

$$
\begin{aligned}
RHS_{reg;2} = -7\kappa r^4 \Big[& \\
& Y_{00}(\alpha_{00}H_{00} + \tfrac{1}{15}[4H_{22}\alpha_{22} + H_{21}\alpha_{21} + 12H_{20}\alpha_{20} + H_{2,-1}\alpha_{2,-1} + 4H_{2,-2}\alpha_{2,-2}]) \\
& + Y_{22}(H_{22}\alpha_{00} + H_{00}\alpha_{22} + \tfrac{1}{14}[H_{21}\alpha_{21} - H_{2,-1}\alpha_{2,-1} - 8H_{22}\alpha_{20} - 8H_{20}\alpha_{22}]) \\
& + Y_{21}(H_{21}\alpha_{00} + H_{00}\alpha_{21} + \tfrac{2}{7}[H_{22}\alpha_{21} + H_{21}\alpha_{22} + H_{2,-2}\alpha_{2,-1} + H_{2,-1}\alpha_{2,-2} + H_{21}\alpha_{20} + H_{20}\alpha_{21}]) \\
& + Y_{20}(H_{20}\alpha_{00} + H_{00}\alpha_{20} + \tfrac{1}{42}[H_{21}\alpha_{21} - 8H_{22}\alpha_{22} + 24H_{20}\alpha_{20} + H_{2,-1}\alpha_{2,-1} - 8H_{2,-2}\alpha_{2,-2}]) \\
& + Y_{2,-1}(H_{2,-1}\alpha_{00} + H_{00}\alpha_{2,-1} + \tfrac{2}{7}[H_{22}\alpha_{21} + H_{21}\alpha_{22} + H_{2,-2}\alpha_{2,-1} + H_{2,-1}\alpha_{2,-2} + H_{20}\alpha_{21} + H_{21}\alpha_{20}]) \\
& + Y_{2,-2}(H_{2,-2}\alpha_{00} + H_{00}\alpha_{2,-2} + \tfrac{1}{14}[H_{2,-1}\alpha_{21} + H_{21}\alpha_{2,-1} - 8H_{20}\alpha_{2,-2} - 8H_{2,-2}\alpha_{20}]) \\
& + Y_{44}\tfrac{1}{2}(H_{22}\alpha_{22} - H_{2,-2}\alpha_{2,-2} + 2H_{22}\alpha_{2,-2} + 2H_{2,-2}\alpha_{22}) \\
& + Y_{43}\tfrac{1}{2}(H_{22}\alpha_{21} + H_{21}\alpha_{22} - H_{2,-1}\alpha_{2,-2} - H_{2,-2}\alpha_{2,-1}) \\
& + Y_{42}\tfrac{1}{14}(H_{21}\alpha_{21} - H_{2,-1}\alpha_{2,-1} + 6H_{22}\alpha_{20} + 6H_{20}\alpha_{22}) \\
& + Y_{41}\tfrac{1}{14}(6H_{21}\alpha_{20} + 6H_{20}\alpha_{21} - H_{22}\alpha_{21} - H_{21}\alpha_{22} - H_{2,-2}\alpha_{2,-1} - H_{2,-1}\alpha_{2,-2}) \\
& + Y_{40}\tfrac{1}{70}(H_{22}\alpha_{22} - H_{21}\alpha_{21} + 18H_{20}\alpha_{20} - H_{2,-1}\alpha_{2,-1} + H_{2,-2}\alpha_{2,-2}) \\
& + Y_{4,-1}\tfrac{1}{14}(H_{22}\alpha_{2,-1} + H_{2,-1}\alpha_{22} - H_{2,-2}\alpha_{21} - H_{21}\alpha_{2,-2} + 6H_{20}\alpha_{2,-1} + 6H_{2,-1}\alpha_{20}) \\
& + Y_{4,-2}\tfrac{1}{14}(6H_{2,-2}\alpha_{20} + H_{20}\alpha_{2,2} + H_{21}\alpha_{2,-1} + H_{2,-1}\alpha_{21}) \\
& + Y_{4,-3}\tfrac{1}{2}(H_{22}\alpha_{2,-1} + H_{2,-1}\alpha_{22} + H_{2,-2}\alpha_{21} + H_{21}\alpha_{2,-2}) \\
& + Y_{4,-4}(H_{22}\alpha_{2,-2} + H_{2,-2}\alpha_{22}) \Big]
\end{aligned}
$$

Now that we have fully calculated the full fourth order approximation, with the exception of the homogeneous coefficients which are handled numerically, we can check our findings against the equation by subtracting every term shown in Table 3.1. Numerical

results of this subtraction in an arbitrary radial direction are shown in Fig 3.1. Dips below the lower boundary line indicate faster convergence at certain discrete points, **perhaps due to the angle at which the point was solved numerically.** However, this result displays the fifth order nature we expected after subtracting out our full fourth order approximation, thus confirming the soundness of our techniques.

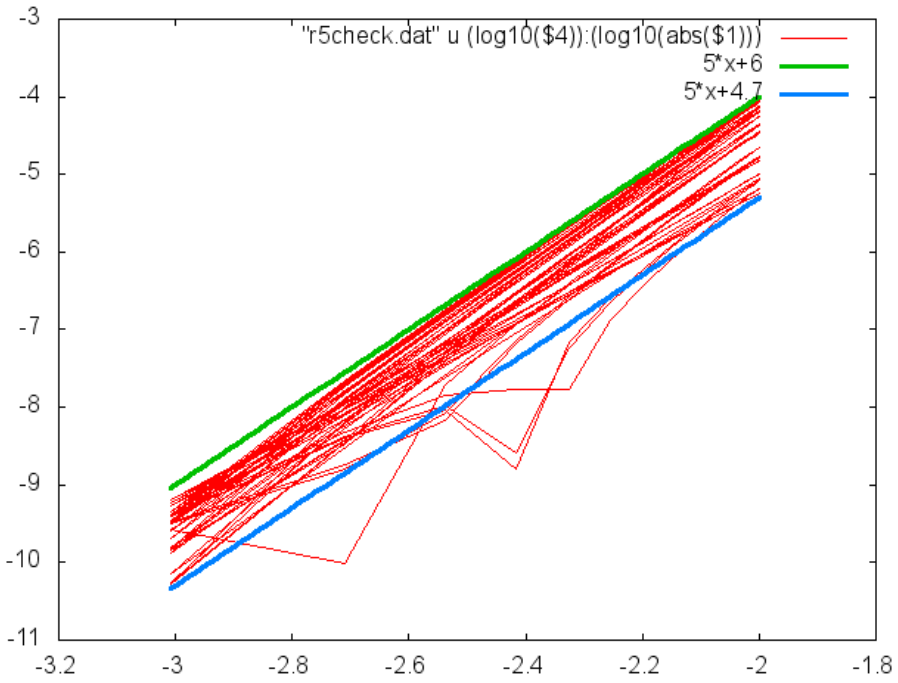

Figure 3.1: Plot showing how the subtraction of our full fourth order calculation shows a fifth order convergence of the solution as we would expect.

In the next chapter we take all of the calculations we have made and automate as much of the processes as we can, while hard coding in a lot of the values we derived. Results from the subtraction method will not only display intuitive images describing the spacetime curvature around a BH, but also error plots portraying the strength of our adapted pseudo spectral-method.

Chapter 4

Adapted Pseudo Spectral-Method Subtracted Approximation

This chapter will outline the remaining structure needed to implement our techniques of manipulating the Hamiltonian and properly managing the irregular components while incorporating the fourth order approximation back into the full numerical solution. First we will outline some of the basic code structure that was needed when adding spherical harmonics as a basis function in place of the standard Fourier component when using pseudo spectral-methods. Next, we will describe an attenuation to our adapted equation to better fit the model solution we expect to resemble. We then plot results for instances of BH's with varying spin and momentum parameters, as well as varying spacial perspectives. Concluding with an error analysis portraying the strength and accuracy of our methods, as well as the limits.

4.1 Code Structure and Subtraction Method

Thus far we have kept all physical parameters and coefficients arbitrary, creating a method which applies to any BH and not just one particular case. Implementing this method required building a list of mode definitions with all necessary products fully accounted for (only up to fourth order). Next we had to adapt the solver to work with the expanded version of the Hamiltonian from EQ 3.1. The code is designed to solve only the regular and homogeneous parts and be supplied with the irregular solution for

the first four orders of r, then resume its normal process after.

The adapted harmonic method we've devised evaluates the Hamiltonian in a series of shells of a specified radial thickness around the black hole singularity at the origin. We specify how many modes we use to solve for the scalar field in each domain as well as how many shells we use. The method captures spatial infinity through a change of variables that compactifies all of space outside the previous shells into the last domain.

Our code makes use of the Inverse Laplacian we derived earlier to solve for the irregular portion of $\bar{u}$ we are concerned with. Instead of solving for $\bar{u}$ directly through the relation

$$\Delta\bar{u} = f(\bar{u}),$$

we solve for the remaining portion of $\bar{u}$ given that we know $\bar{u}_{irreg}$ and RHS_{irreg}. The equation above is equivalent to the following.

$$\Delta(\bar{u}_{num} + \bar{u}_{sub}) = f_{num}(\bar{u}) + f_{sub}(\bar{u}).$$

where $\bar{u}_{num}$ and $\bar{u}_{sub}$ are the remaining part of $\bar{u}$ to be determined numerically and the subtracted irregular component of $\bar{u}$ up to fourth order after taking the Inverse Laplacian.

This adapted method pushes a few bounds numerically in terms of convergence. In order to arrive at a solution that fit the model, we attenuate the equation within our solver's structure by a set of guidelines described in the next section.

4.2 Attenuation

We want to build an attenuation function that fits the following criteria: one that peaks to one at the origin ($r = 0$) with a slope of 1, and drops off to zero quickly and smoothly. Attenuating helps to smooth out the "jumps" when transitioning between the shells that build up our domain and also to provide a guide to tame our adapted solution to better fit our data to the known PSM solution. Thus, we do not subtract the actual polynomial/spherical harmonic terms from the RHS. Nor, however, do we subtract purely attenuated ones. Instead, we follow the following set of steps. Beginning from an irregular RHS mode in the form $r^n Y_{lm}$, we calculate the inverse Laplacian

exactly:

$$u_{irreg} = \nabla^{-2}(r^n Y_{lm}) = \frac{1}{(n+2)(n+3) - l(l+1)} r^{n+2} Y_{lm}$$

We then attenuate by dividing through by an expression we'll write in the form

$$\begin{aligned} p &\equiv 1 + \alpha r^3 + \beta r^4 + a r^5 + b r^6 + c r^7 + d r^8 \\ u_{att} &\equiv \frac{u_{irreg}}{p} = \frac{1}{(n+2)(n+3) - l(l+1)} \frac{r^{n+2}}{1 + \alpha r^3 + \beta r^4 + a r^5 + b r^6 + c r^7 + d r^8} Y_{lm} \end{aligned}$$

In the limit of large r, we find

$$\begin{aligned} u_{att} &\approx \frac{d^{-1}}{(n+2)(n+3) - l(l+1)} r^{n-6} Y_{lm} \\ R_{att} \equiv \nabla^2 u_{att} &= d^{-1} \frac{(n-6)(n-7) - l(l+1)}{(n+2)(n+3) - l(l+1)} r^{n-8} Y_{lm} \end{aligned}$$

This should be numerically tractable. In the limit of small r, we find

$$u_{att} \approx \frac{1}{(n+2)(n+3) - l(l+1)} Y_{lm} \left[r^{n+2} - \alpha r^{n+5} - \beta r^{n+6} + O(r^{n+8}) + ... \right]$$

$$R_{att} \approx r^n Y_{lm} - \alpha \frac{(n+5)(n+6) - l(l+1)}{(n+2)(n+3) - l(l+1)} r^{n+3} Y_{lm} - \beta \frac{(n+6)(n+7) - l(l+1)}{(n+2)(n+3) - l(l+1)} r^{n+4} Y_{lm} + O(r^{n+6}) + ...$$

Here, the first term is the one we wish to cancel, but we add in additional modes. Note that since we are canceling *irregular* modes, the α term, containing an extra r^3, is regular and does not cause problems for convergence. The β term, containing an r^4 contribution, is irregular, but first arises at fifth order in r, and thus we do not attempt to cancel out its contribution.

4.3 Scalar Field Results

Testing our code for ranging spacial and physical characteristics give us a good sense of the successes of our method as well as some interesting looks at the scalar field showing the gravitational potential. Below are plots describing BHs with varying spin

and momentum conditions and plotted in several different spacial regimes. By taking the negative of the scalar field, the figures display the intuitive nature of a BH drawing in the space around it. The plots show the significant effects expected around the singularity and asymptotic behavior of the potential observed away from the object. Only 4.1 has a ranging z-coordinate, while the other figures have a fized z-value.

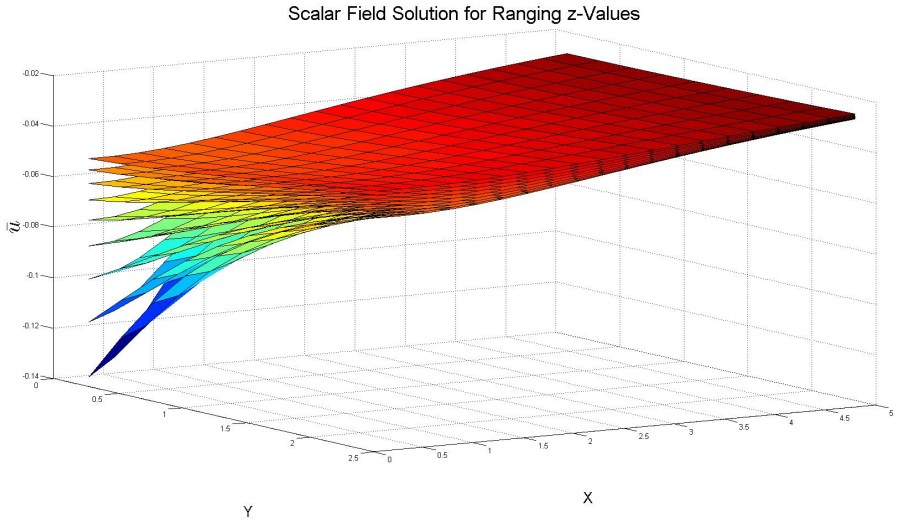

Figure 4.1: By overlaying surface plots for the scalar field solution, we were able to see an almost 3-dimensional effect of a BH on the spacetime around it. All values of z are positive and the plot shows that the gravitational effects are more dramatic, not only moving closer to the BH in the x-y plane, but also in the z direction.

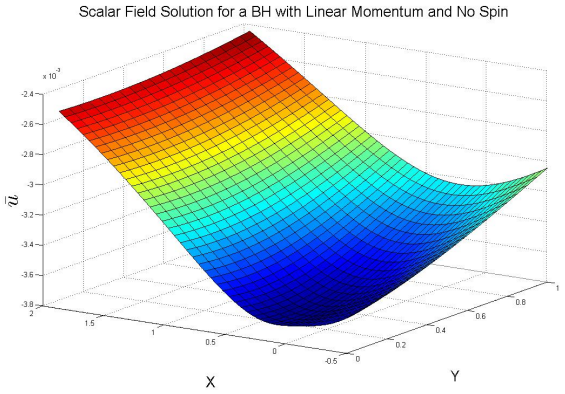

Figure 4.2: BH with momentum and no spin

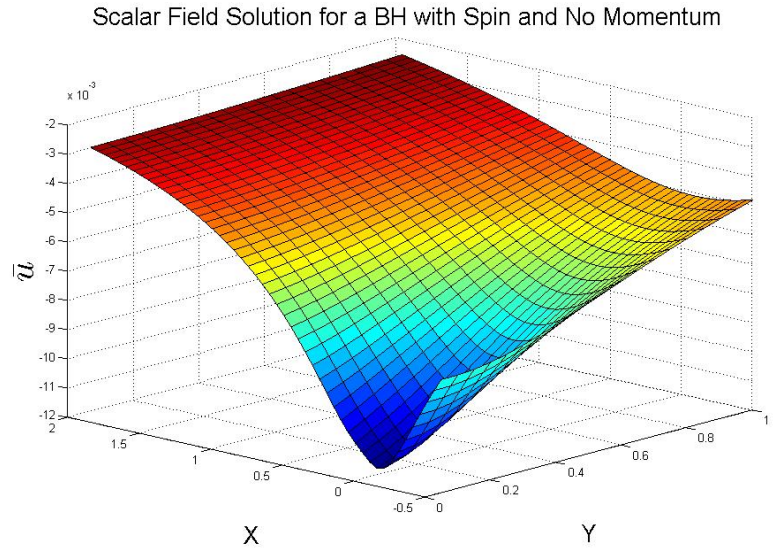

Figure 4.3: BH with spin and no momentum

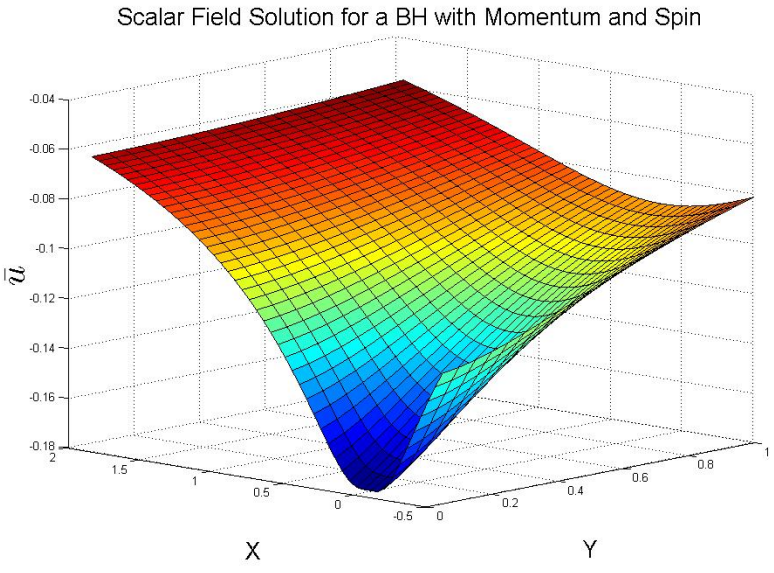

Figure 4.4: BH with spin and momentum components

4.4 Error Analysis

Tracking error in any numerical process is a key component to understanding, not only how well the method performed, but also how to interpret the data project how to optimize results. We calculated the error for the cases shown in the last section for BHs with varying spin and momentum components. We took our numerical solution and tested it with a five-point fourth-order Laplacian stencil, which acted on a grid with multiple levels of refinement.

The test was designed to see how well our solution did with a fourth order Laplacian operator acts on it, and compare this result to the RHS of the Hamiltonian equation. We took the absolute value of the difference between the RHS and fourth-order Laplacian at the collocation point locations from our code. The fourth-order five-point Laplacian in the x-direction

$$D_{xx} = \left[-\frac{1}{12} f(x-2h,y,z) + \frac{4}{3} f(x-h,y,z) - \frac{5}{2} f(x,y,z) + \frac{4}{3} f(x+h,y,z) - \frac{1}{12} f(x+2h,y,z) \right] /h^2$$

is the stencil we used in our error analysis within the domain shown in Fig. 4.5.

The grid shown in Fig. 4.5 is a 2D projection of the actual grid we used, which followed this same pattern in in three dimensions. Here, we only track points needed for calculation. This leaves us with clusters around the points we are interested in and leaving the out any diagonal elements that would result from stepping through more than one direction at a time in our differencing stencil. This method prevents the code from being bogged down with extra calculation and storage while computing the solution at each point. The refinement method we chose shrunk the spacing used in the Laplacian stencil by half each iteration. Since we have chosen fourth-order precision and refine by a factor of 2 each iteration, we expect to drop the error by a factor of 2^4 after each level of refinement.

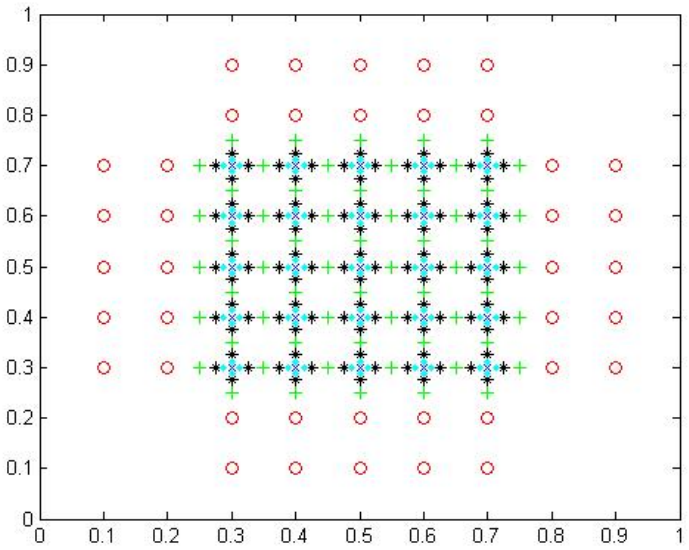

Figure 4.5: Here we have a 2D slice of our test domain showing the grid refinement method we implemented. The points we are solving for are the 5x5 "x's" in the middle of each cluster of points. The red "o's" are ghost points needed for the fourth-order five point Laplacian calculation and are the same distance away from an "x" as another "x". This grid layout shows three levels of refinement. The first level of refinement is shown as the green "+'s", the next level has black "*'s" and the third level has blue dots.

4.5 Error Results

The following figures will display the results of our error analysis on BHs with different physical characteristics and numerical levels of refinement. The plots will show the systematic limits of our method, numerical noise caused by round off error, as well as varying the number of modes used to resolve the numerical solution.

The order the plots are in relate to the order in which we calculated them and mention how each one is significant in the scheme of finding error bounds and reasons for anomalies.

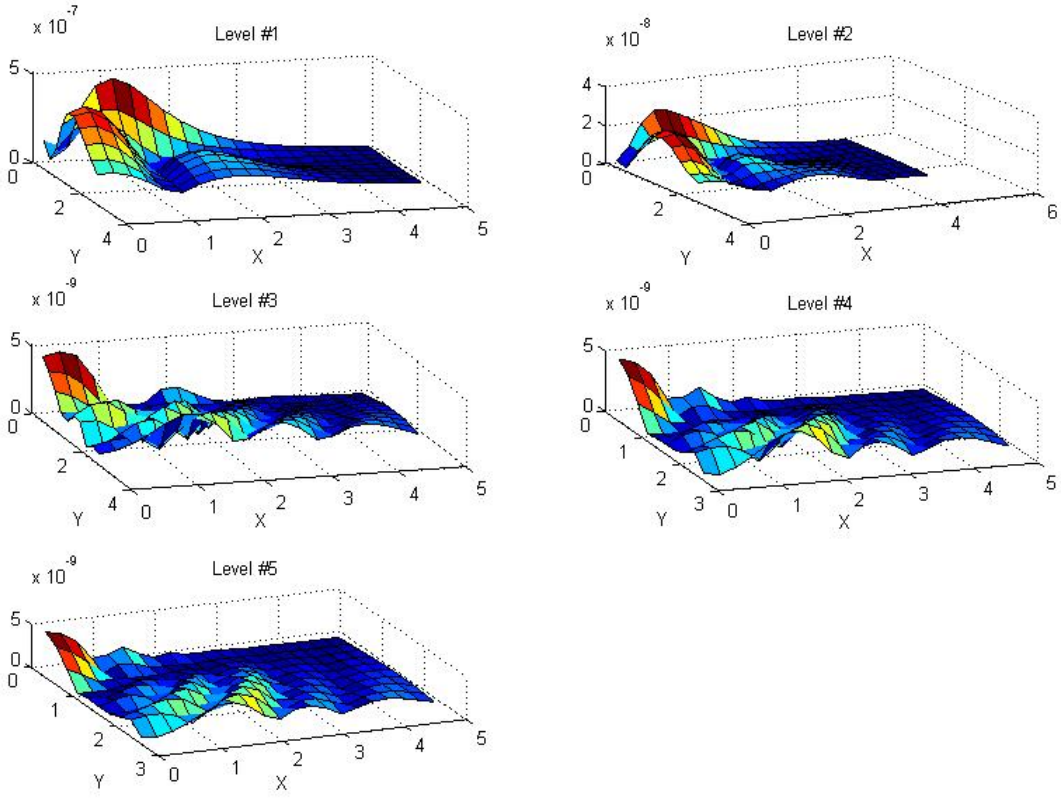

Figure 4.6: This figure shows the shape of the error in a 2D mesh. Here we calculated the absolute value of the difference between the right hand side value and the Laplacian of our computed solution as we refine our grid, level by level. The errors shown here correspond to the solution plotted in Fig 4.1 with the singularity in the top left corner. As mentioned at the beginning of the paper, we notice that the error values display a Gibbs phenomena appearance in a radial domain as ripples in the structure, spiking at the singularity. The phenomena is a little distorted since the plot takes the absolute value of the error into account.

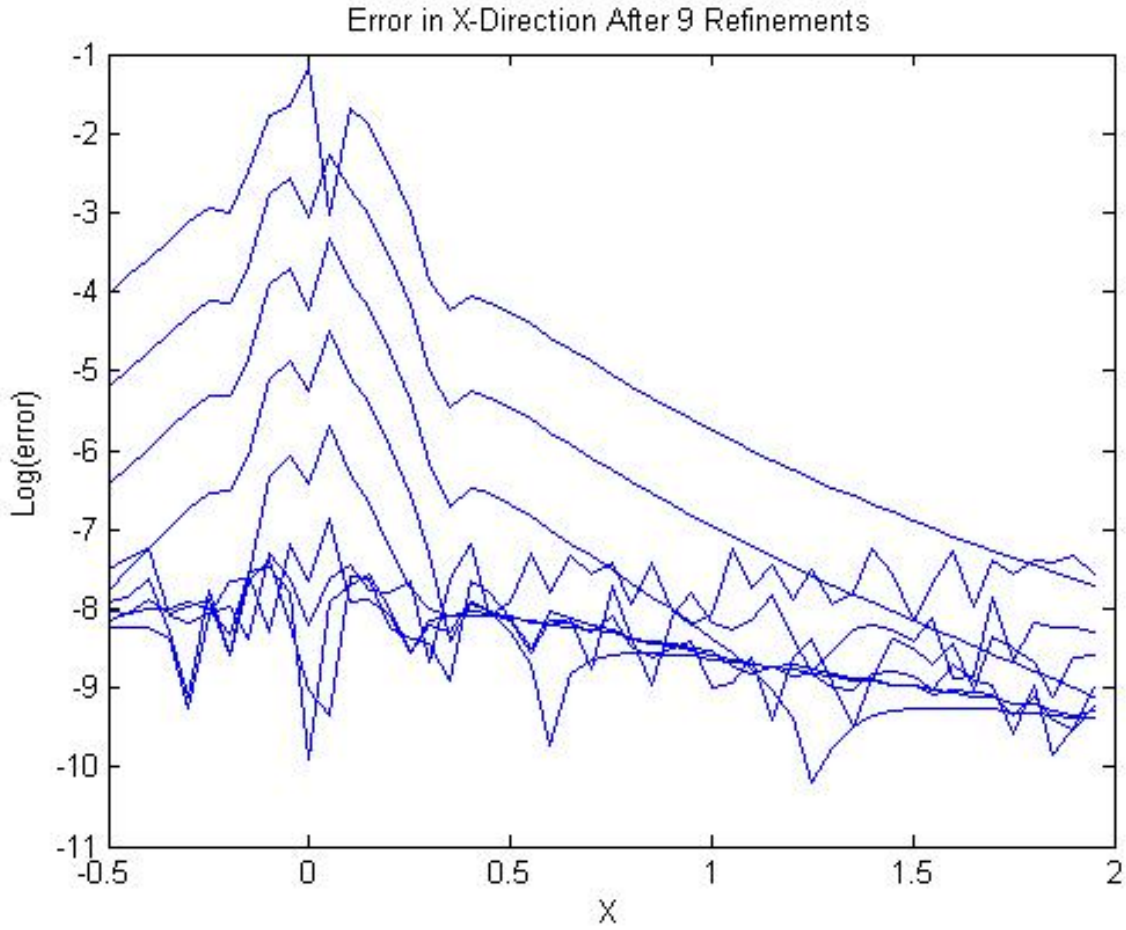

Figure 4.7: Log of the error in the x-direction for a BH with momentum and spin. This is a high resolution run in which 12 domains were used to calculate the solution. The systematic noise began to effect the numerical accuracy heavily at the fifth level of refinement, capping our accuracy limit to $\approx 10^{-8}$. The round off error continues to worsen as more refinement is put on the solution, thus revealing the optimal level given our spacing selection. For the other spin and momentum cases, the error bounds are pushed much lower. Since the x-values transverse over the BH we see this error spike at $x = 0$ around the singularity, and smoother, exponential convergence away from it.

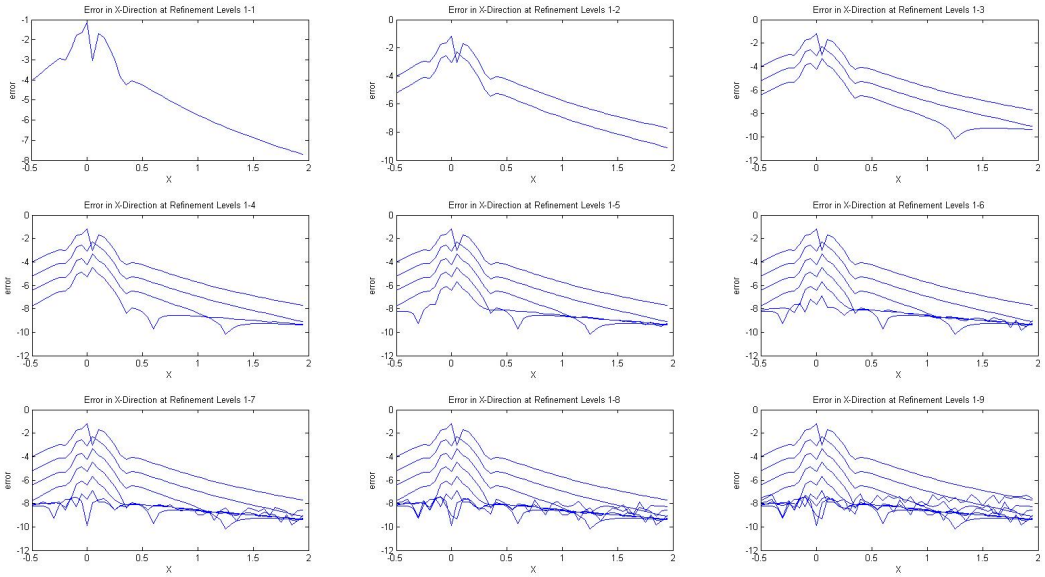

Figure 4.8: This plot again shows the error in the x-direction for a BH with spin and momentum, but displays how Fig. 4.7 was reached after successive refinement levels. The systematic error bound appears to be $\approx 10^{-8}$.

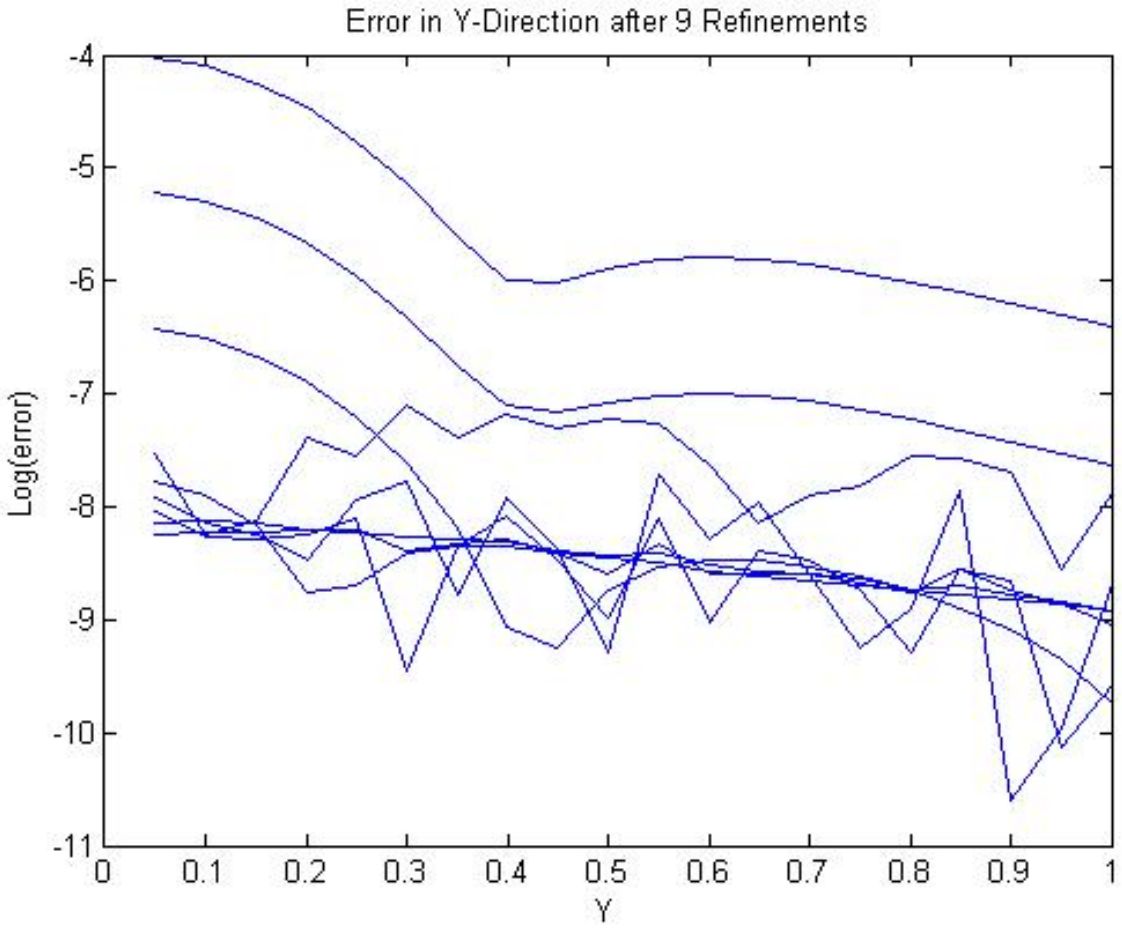

Figure 4.9: Log of the error in the y-direction shown in reference to the solution plotted in Fig. 4.2 with spin and momentum. This is a high resolution run.

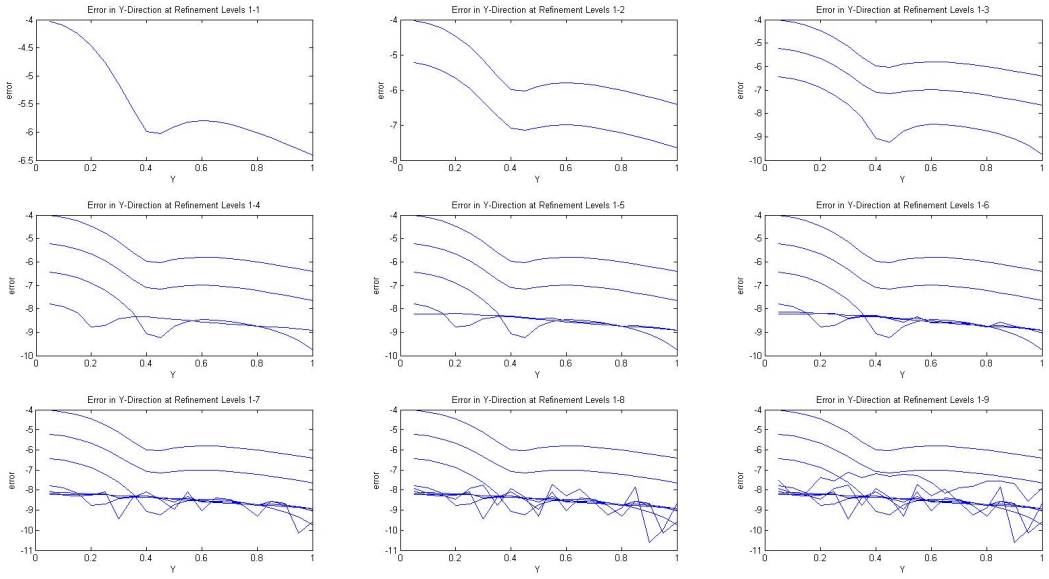

Figure 4.10: This plot again shows the error in the y-direction for a BH with spin and momentum, but displays how Fig. 4.9 was reached after successive refinement levels. The systematic error bound in the y-direction also appears to be $\approx 10^{-8}$.

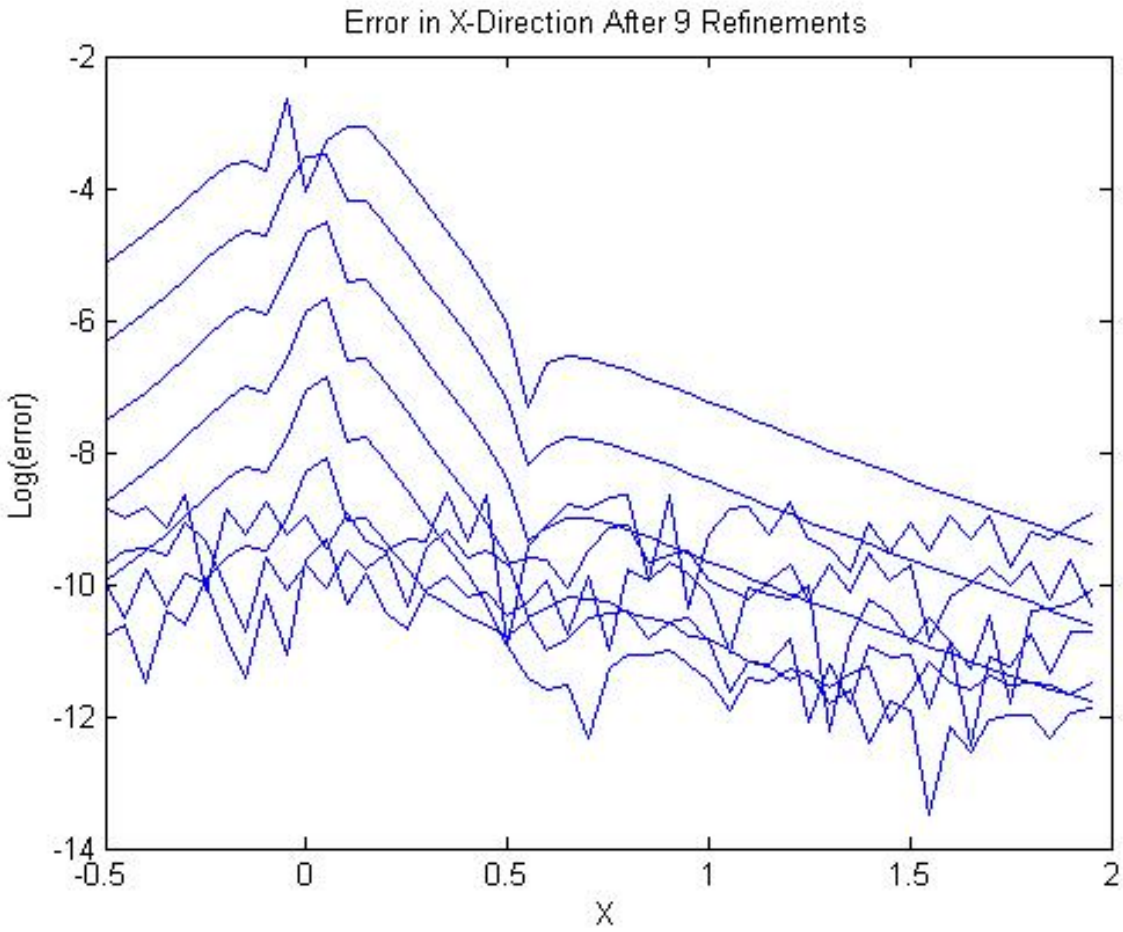

Figure 4.11: Log of the error in the x-direction shown in reference to the solution plotted in Fig. 4.3 with no momentum. This is a high resolution run.

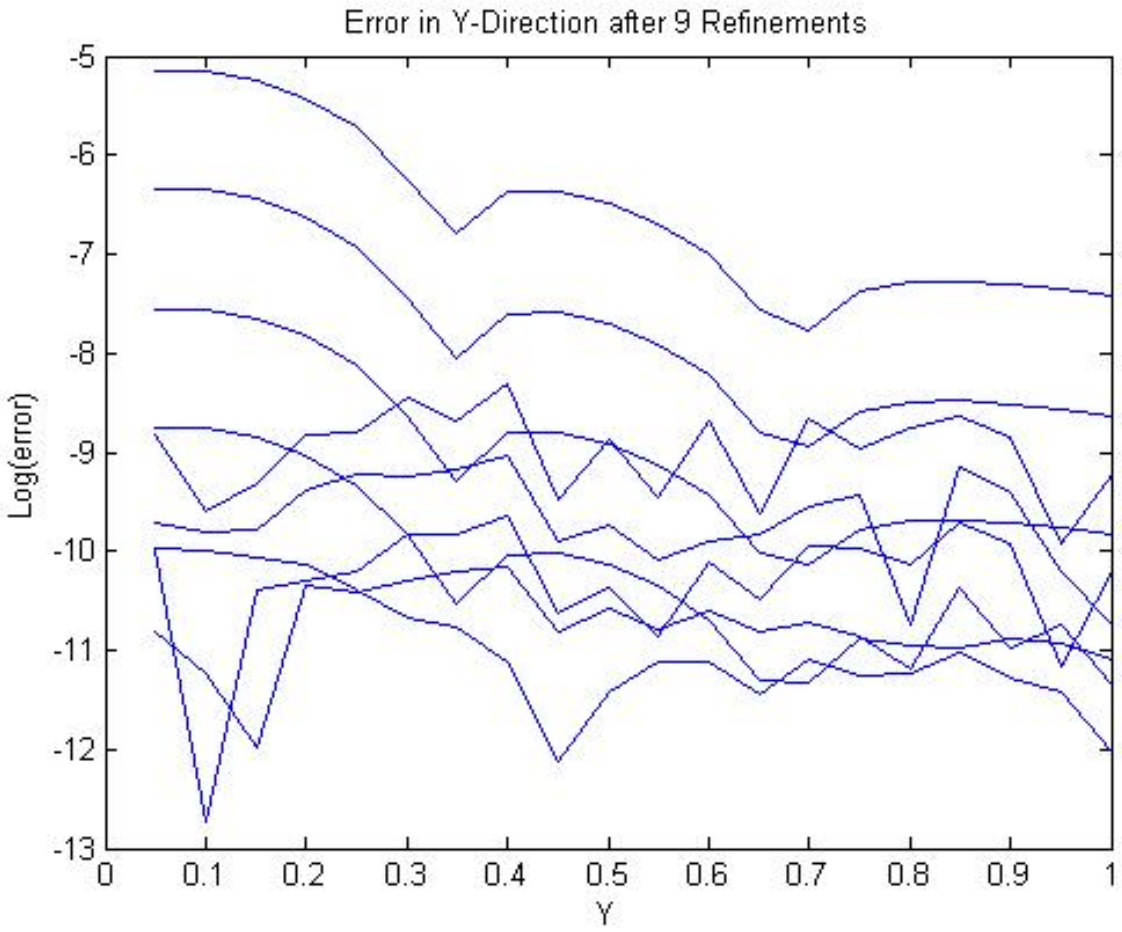

Figure 4.12: Log of the error in the y-direction shown in reference to the solution plotted in Fig. 4.3 with no momentum. This is a high resolution run.

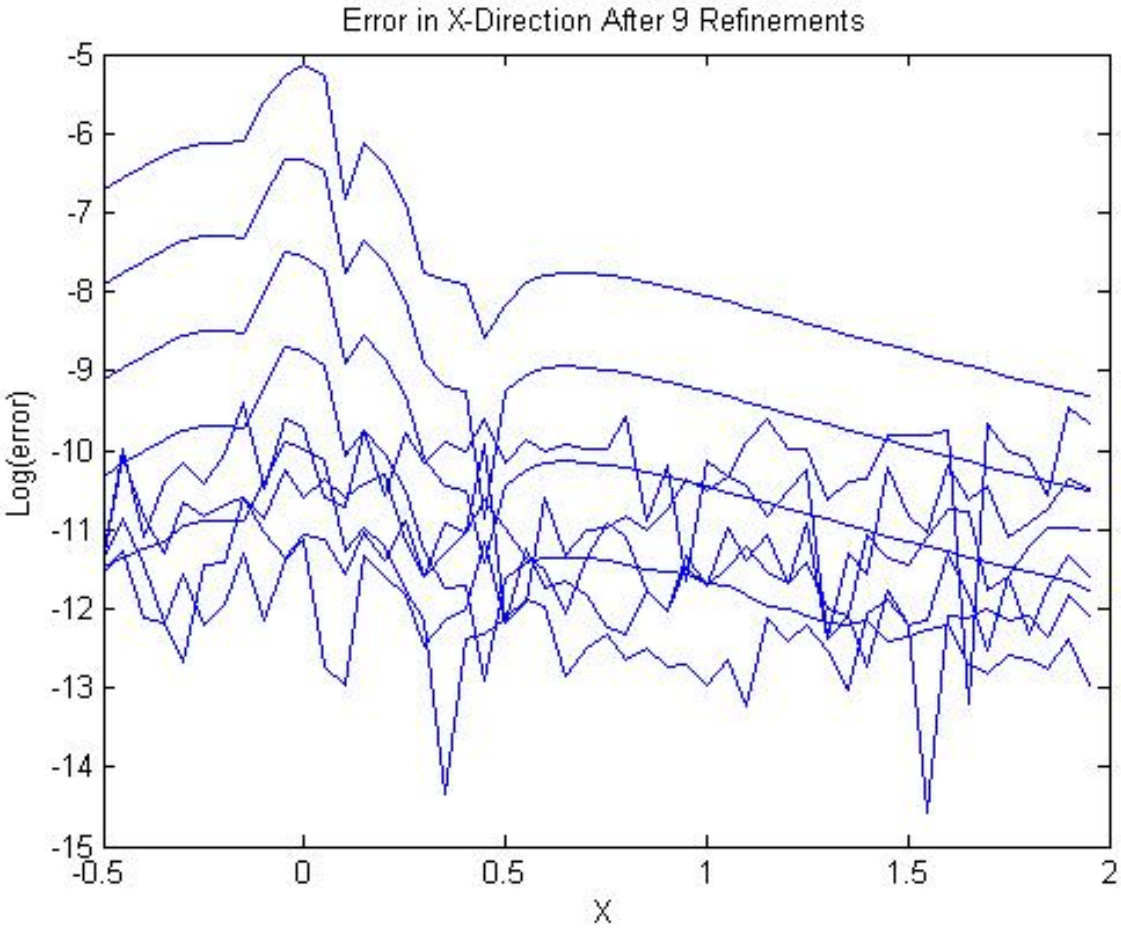

Figure 4.13: Log of the error in the x-direction shown in reference to the solution plotted in Fig. 4.4 with no spin. This is a high resolution run.

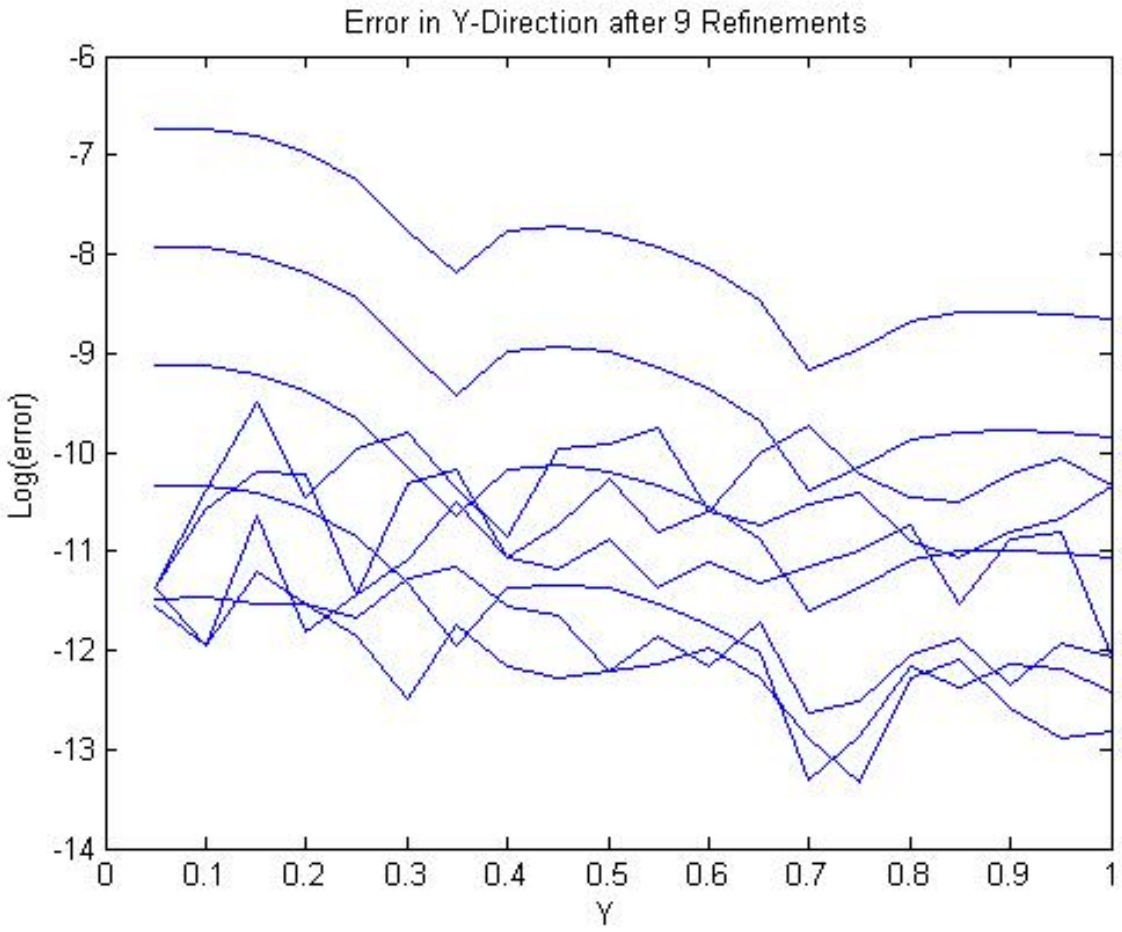

Figure 4.14: Log of the error in the y-direction shown in reference to the solution plotted in Fig. 4.4 with no spin. This is a high resolution run.

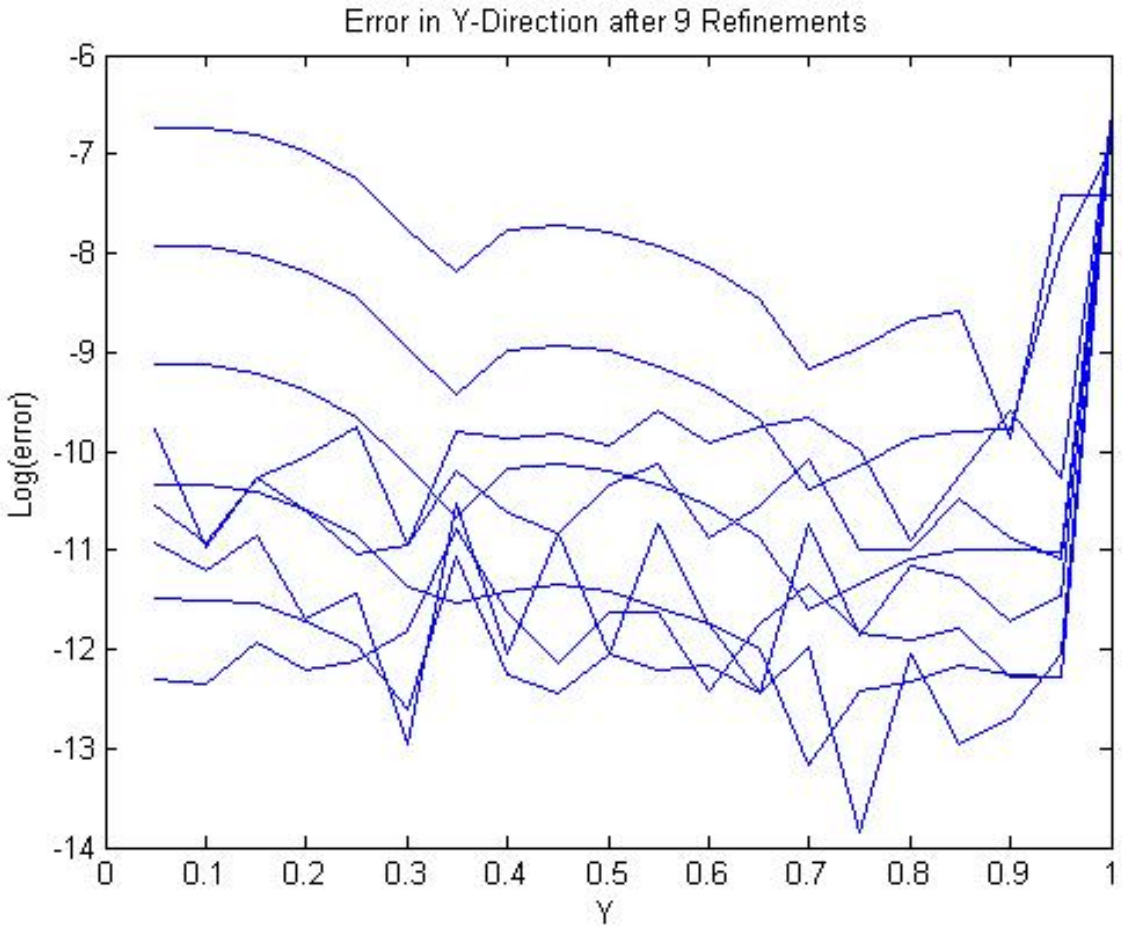

Figure 4.15: When testing our the method with low resolution, using 10 shell domains and 17 modes per domain, the solution was poorly handled and caused a huge jump in the data when transferring into the last shell at around $r = 1$, which had to account for the entirety of space outside of the other shells. We saw the same anomaly testing in the x-direction as well.

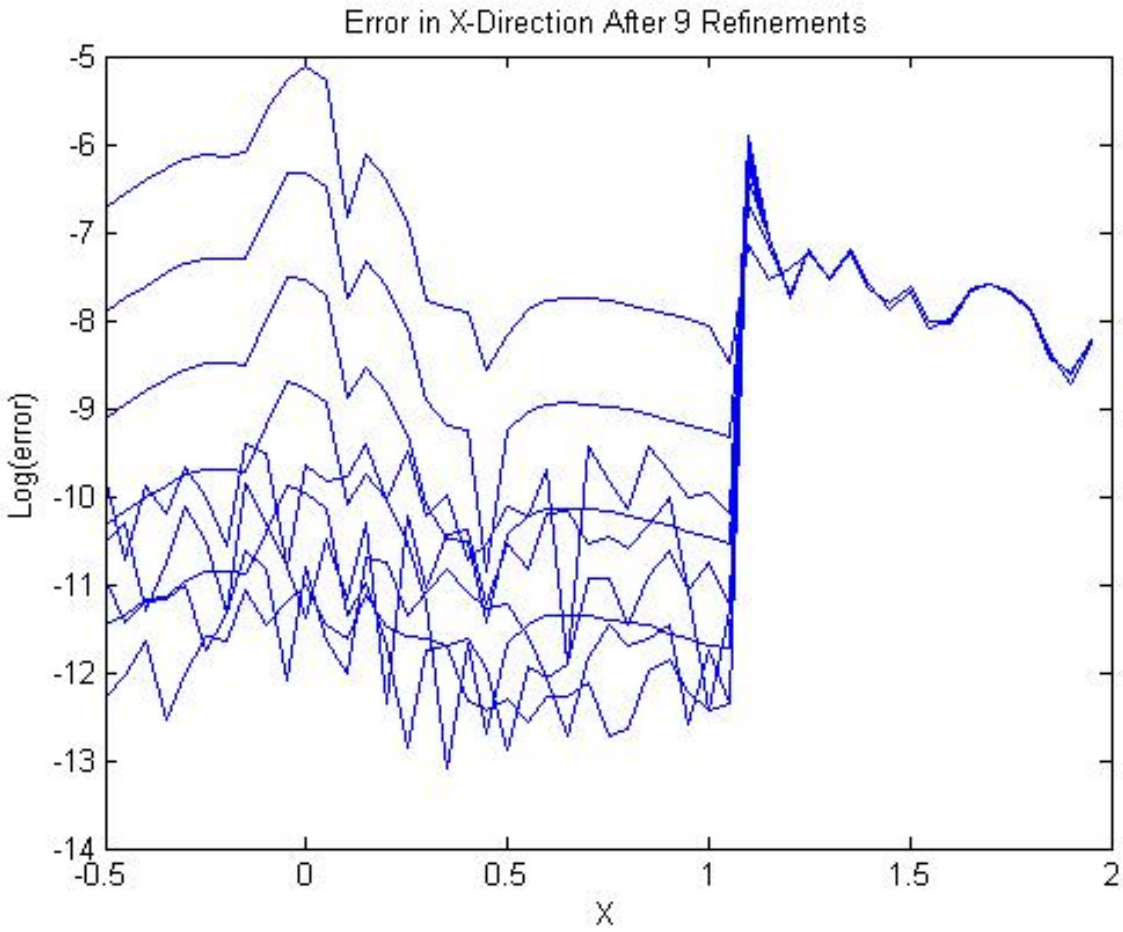

Figure 4.16: Low resolution jump in the data when transferring into the last shell at around $r = 1$.

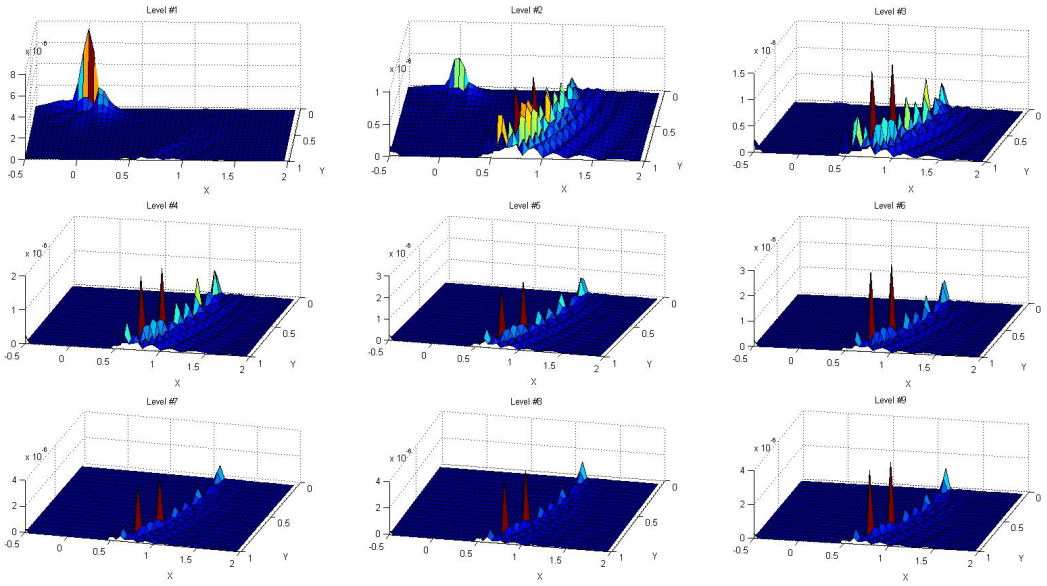

Figure 4.17: Surface plot of the error caused by the low resolution data shown in Figs. 4.15 & 4.16. Notice the radial distribution of the error. Gibbs phenomena may also be seen in this figure.

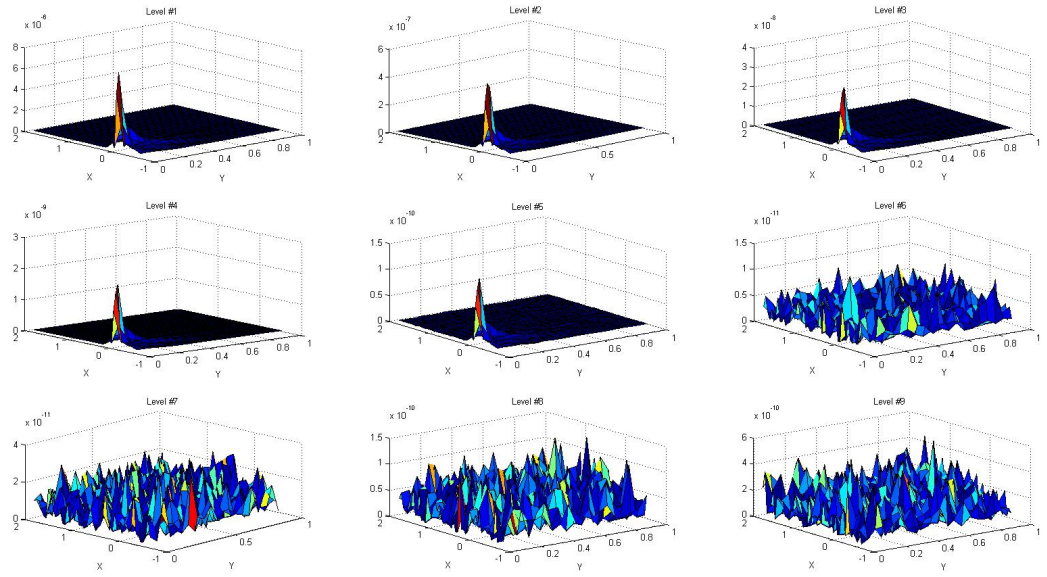

Figure 4.18: By allowing for more modes to represent the solution in our code, we were able to resolve the issues caused when transferring into the last shell domain; resulting in plots similar to the high resolution cases. We can see the error saturation starting at the sixth refinement level.

Chapter 5

Conclusions

We were successful in our attempt to numerically handle a fourth order approximation for the irregular component of the scalar field to better resolve errors around the singularity. We can reach systematic error bounds with only a few tractable mesh refinements and optimize our methods with this process.

A fourth-order account for irregularities turned out to be an excellent candidate for this method. Looking ahead at the next orders of r to consider, the error bounds we met will not improve much given the added treatment of these extra terms since we were reaching saturation in our differencing scheme fairly quickly using fourth order. Considering higher order approximations will also require much additional treatment in the tracking of the irregular coefficients from the nonlinear portions of the Hamiltonian, EQ. 3.6. However, extending the method to higher order approximations is indeed plausible.

We may improve the standing method by doing selective refinements, namely refine the area near the singularity more than the rest of the domain. Since we reach the systematic limits faster away from the BH and produce a lot of noise trying to get the same resolution at the BH, it might be worth adjusting this method to allow for multiple scales of mesh refinement. Furthermore, an extension to include a second BH would only involve one more fourth order term, making it very tractable numerically. If one wished to include n BHs, one would have to account for a cross terms of each pairing of the objects, resulting in $\frac{n(n+1)}{2}$ additional fourth order terms.

Bibliography

[1] Marcus Ansorg, Bernd Brügmann, and Wolfgang Tichy. Single-domain spectral method for black hole puncture data. *Physical Review D*, 70(6):064011, 2004.

[2] Steven Brandt and Bernd Brügmann. A simple construction of initial data for multiple black holes. *Physical Review Letters*, 78(19):3606, 1997.

[3] Eric Gourgoulhon, Philippe Grandclement, Keisuke Taniguchi, Jean-Alain Marck, and Silvano Bonazzola. Quasiequilibrium sequences of synchronized and irrotational binary neutron stars in general relativity: Method and tests. *Physical Review D*, 63(6):064029, 2001.